



## **Six New Species of *Labeotropheus* (Cichliformes: Cichlidae) from the Malaŵian Shore of Lake Malaŵi, Africa**

Authors: Pauers, Michael J., and Phiri, Titus B.

Source: Ichthyology & Herpetology, 111(2) : 264-292

Published By: The American Society of Ichthyologists and Herpetologists

URL: <https://doi.org/10.1643/i2021055>

---

BioOne Complete ([complete.BioOne.org](https://complete.BioOne.org)) is a full-text database of 200 subscribed and open-access titles in the biological, ecological, and environmental sciences published by nonprofit societies, associations, museums, institutions, and presses.

Your use of this PDF, the BioOne Complete website, and all posted and associated content indicates your acceptance of BioOne's Terms of Use, available at [www.bioone.org/terms-of-use](https://www.bioone.org/terms-of-use).

Usage of BioOne Complete content is strictly limited to personal, educational, and non-commercial use. Commercial inquiries or rights and permissions requests should be directed to the individual publisher as copyright holder.

---

BioOne sees sustainable scholarly publishing as an inherently collaborative enterprise connecting authors, nonprofit publishers, academic institutions, research libraries, and research funders in the common goal of maximizing access to critical research.

## Six New Species of *Labeotropheus* (Cichliformes: Cichlidae) from the Malawian Shore of Lake Malaŵi, Africa

Michael J. Pauers<sup>1,2</sup> and Titus B. Phiri<sup>3,4</sup>

***Labeotropheus* is a small genus of rock-dwelling haplochromine cichlid fishes endemic to Lake Malaŵi in the Great East African Rift Valley. As currently recognized, *Labeotropheus* contains five species: *L. artatorostris*, *L. chlorosiglos*, *L. fuelleborni*, *L. simoneae*, and *L. trewavasae*. Despite increased recent attention from taxonomists, there are still several undescribed species within this genus. Here, based upon morphological and meristic data, as well as differences in male nuptial color pattern, we describe six new species. Additionally, we update the type locality of *L. simoneae*. The descriptions of these new species are in line with current recommendations to better define and delimit the taxonomy of cichlids from Lake Malaŵi, which will hopefully lead to increased efforts to conserve these fishes.**

LAKE Malaŵi, the southernmost lake of the Great East African Rift Valley, is home to the most diverse radiation of vertebrate life in the world, hosting an estimated 1,000 or more species of endemic cichlid fishes (Sayer et al., 2019). Perhaps not surprisingly, this lake and these remarkable fishes have been favorite study subjects for those seeking to understand the causes of this unparalleled burst of evolution, as well as those who would document and describe the diversity of these fishes (Weyl et al., 2010). What is surprising is that, after almost a century of taxonomic study, new species continue to be described. In the three years preceding this study, 14 species have been described in seven published papers (Dierickx et al., 2018; Oliver, 2018; Stauffer, 2018; Stauffer et al., 2018; Dierickx and Snoeks, 2020; Stauffer et al., 2020; Stauffer and Konings, 2021), and the consensus among experts is that many more species of cichlid from Lake Malaŵi await description (Kanyerere et al., 2019).

The most diverse assemblage of cichlids is restricted to the shallow nearshore areas of Lake Malaŵi (Ribbink et al., 1983a; Kanyerere et al., 2019). The cichlid fauna of this habitat is dominated by the rock-frequenting haplochromines known by the Chitonga name ‘mbuna.’ The mbuna consist of 13 genera of brightly colored, highly stenotopic fishes, notable for the extensive genetic, morphological, and behavioral divergence among allopatric populations (Ribbink et al., 1983a; Oliver and Arnegard, 2010; Pauers and McMillan, 2015; Conith et al., 2020). While some of these genera have received extensive attention from ichthyologists, with numerous species having been added since Ribbink et al.’s (1983a) survey of these fishes, others remain in need of taxonomic attention (Pauers, 2010).

The genus *Labeotropheus* is one genus of the mbuna common to the rocky nearshore areas of Lake Malaŵi, and has, until recently, been overlooked by taxonomists (Pauers, 2010). It is distinguished from the other mbuna due to a steeply sloping head; broad, fleshy snout; wide jaws with retrognathous lower jaw; and an inferior and subterminal mouth (Oliver and Arnegard, 2010). First described by Ahl in

1927, *Labeotropheus* had long been considered to contain only two species, *L. fuelleborni* and *L. trewavasae*, despite extensive evidence suggesting the existence of numerous species within this genus (Ribbink et al., 1983a, 1983b; Pauers, 2010). While recent efforts have added three additional species (*L. chlorosiglos* and *L. simoneae*, Pauers, 2016; *L. artatorostris*, Pauers, 2017), the presence of other allopatric and uniquely colored populations of *Labeotropheus* suggests the existence of yet more species of this genus.

Within *Labeotropheus*, a useful first criterion to employ when identifying and describing species is the ratio of body depth to body length (Fryer, 1956; Pauers, 2016). Quantifying this ratio is the first step in distinguishing robust species from slender species (Pauers and McMillan, 2015), especially if they are sympatric with one another (*sensu* Stauffer and McKaye, 2001). Typically, the robust *Labeotropheus* (e.g., *L. fuelleborni*, *L. artatorostris*) have a ratio of body depth to standard length that is greater than or equal to 35%, while that of slender species (e.g., *L. trewavasae*, *L. simoneae*) is less than or equal to 30%; additionally, there are species with intermediate body depth–standard length ratios (e.g., *L. chlorosiglos*; Pauers, 2016). Once a putative new species has been assigned to the robust, intermediate, or slender morphotype, other criteria, especially male nuptial coloration and craniofacial features (i.e., snout length, snout pad length, rostral length, length of the upper and lower jaws, etc.; Pauers, 2016) become useful for diagnosing new species.

Here, based upon specimens collected during the course of two expeditions conducted with the express purpose of documenting the distribution and diversity of *Labeotropheus*, we present the descriptions of six new species.

### MATERIALS AND METHODS

**Study sites.**—We conducted two expeditions in Lake Malaŵi, one from 29 July to 3 August 2018, and the other from 11 to 20 January 2020. During the 2018 expedition, we obtained specimens from seven locations surrounding the Luromo Peninsula along the northwestern shore of the lake. In 2020,

<sup>1</sup> Milwaukee Public Museum, Section of Vertebrate Zoology, 800 W. Wells Street, Milwaukee, Wisconsin 53233; Email: mjpauers@gmail.com. Send correspondence to this address.

<sup>2</sup> University of Wisconsin-Milwaukee at Waukesha, Department of Mathematics and Natural Sciences, 1500 N. University Drive, Waukesha, Wisconsin 53188.

<sup>3</sup> Senga Bay Fisheries Research Centre, P.O. Box 316, Salima, Malaŵi; Email: titobandulo@gmail.com.

<sup>4</sup> National Aquaculture Centre, Domasi, Malaŵi, P.O. Box 44, Zomba, Malaŵi.

Submitted: 9 May 2021. Accepted: 23 February 2023. Associate Editor: R. E. Reis.

© 2023 by the American Society of Ichthyologists and Herpetologists DOI: 10.1643/i2021055 Published online: 25 May 2023

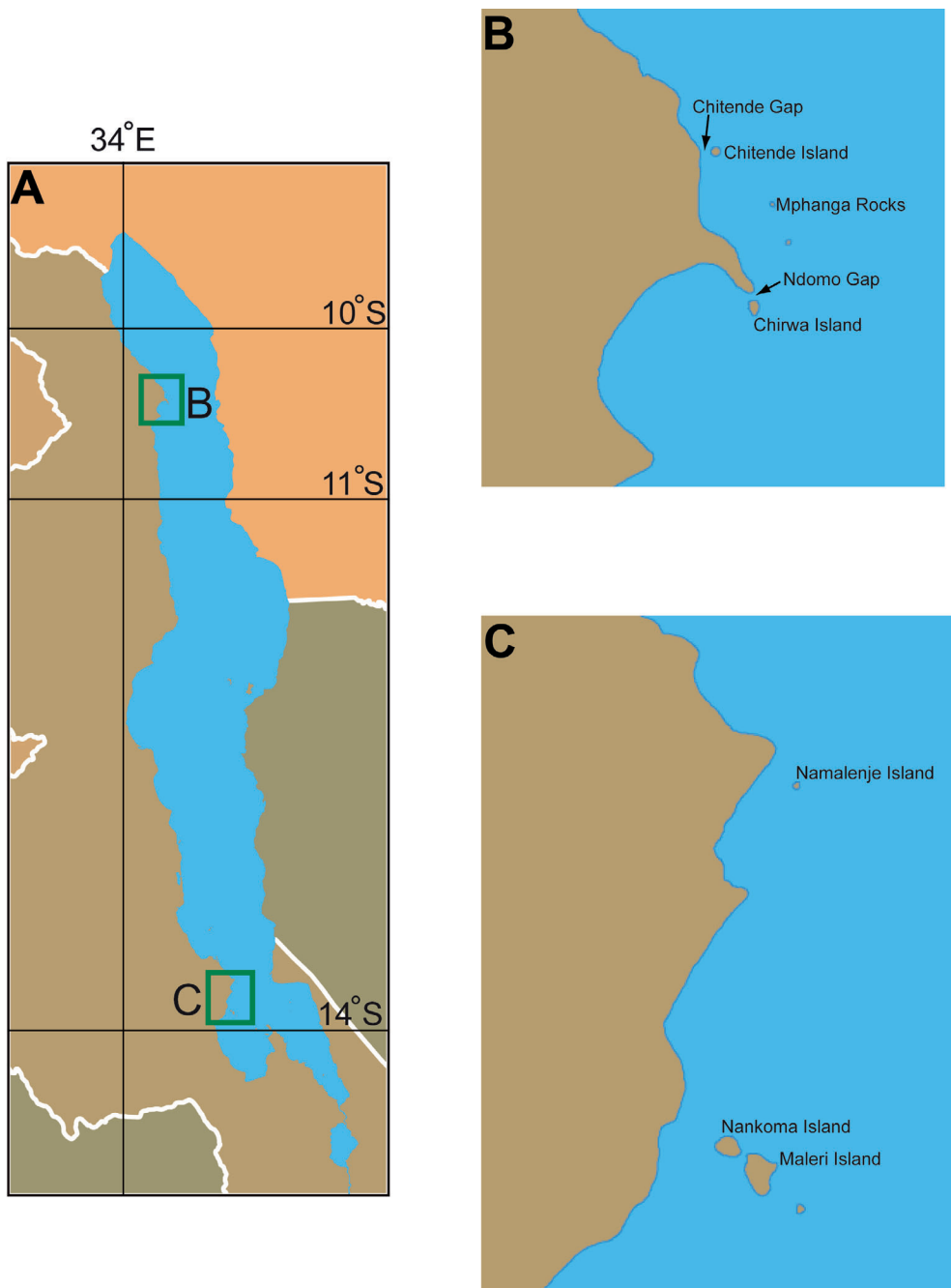


**Fig. 1.** Maps of Lake Malaŵi indicating locations where specimens of *Labeotropheus* were collected. (A) Lake Malaŵi; (B) locations visited in 2018, near the Luromo Peninsula in the northwestern portion of the lake; (C) locations visited in 2020, in the southwestern portion of the lake.

we visited three locations in the southwestern portion of Lake Malaŵi, including the Lake Malaŵi National Park. All sampling locations are shown on the map in Figure 1, and the GPS coordinates are found in Table 1.

**Permits.**—For the 2018 expedition, permission to conduct research on Lake Malaŵi was granted by the National Commission for Science and Technology of Malaŵi on 30 July 2018; there was no permit or reference number issued on this document. Permission to export specimens from Lake Malaŵi to the United States was granted by the Malaŵi Department of Fisheries on 4 August 2018 (reference no. DOFI/20/4/8). The United States Fish and Wildlife Service granted permission to import the specimens to the U.S. on 19 July 2018 (confirmation no. 2018DU2260473).

For the 2020 expedition, permission to conduct research on Lake Malaŵi was granted by the National Commission for Science and Technology of Malaŵi on 14 January 2020 (reference no. NCST/RTT/1/20). Permission to collect specimens from the waters of Lake Malaŵi National Park was issued on 14 January 2020; there is no permit or reference number issued on this document. Permission to export specimens from Lake Malaŵi to the United States was granted by the Malaŵi Department of Fisheries on 19 January 2020 (reference no. DF/019/200). The United States Fish and Wildlife Service granted permission to import the specimens to the U.S. on 12 December 2019 (confirmation no. 2019CH2529841).

The research activities involving live vertebrate animals that occurred during both of these expeditions were approved by the Institutional Animal Care and Use Com-

**Table 1.** Locations where *Labeotropheus* were obtained.

| Year | Location         | GPS coordinates  |
|------|------------------|--|
| 2018 | Chitende Island  | -10.3982807, 34.2579842  |
| 2018 | Chitende Gap     | -10.3975493, 34.2560859  |
| 2018 | Mphanga Rocks    | -10.4328123, 34.2783040  |
| 2018 | Chirwa Island    | -10.4684007, 34.2811572  |
| 2018 | Ndomo Gap        | -10.4350479, 34.2643444  |
| 2020 | Namalenje Island | -13.730081, 34.641074<br>-13.730788, 34.640388<br>-13.729377, 34.640478<br>-13.730081, 34.641074 |
| 2020 | Maleri Island    | -13.8840189, 34.6118803<br>-13.9089591, 34.6260792<br>-13.8926036, 34.6221075                    |
| 2020 | Nankoma Island   | -13.8840189, 34.6118803  |

mittee of the University of Wisconsin-Milwaukee under Animal Care and Use Protocol 17-18#44.

**Specimens.**—All specimens were captured by divers who chased the fishes into monofilament gillnets. Upon capture, the fishes were photographed while alive before being euthanized with an overdose of MS-222; a dosage of approximately 250 mg/L was used to euthanize the fish. Once euthanized, the right pelvic fin was removed with scissors and placed into 95% ethanol (EtOH) for preservation and possible future genetic analyses; the remaining whole-body specimen was given an identification number and fixed in 10% buffered formalin for 48–72 hours. After fixation, the fishes were prepared for transport to the Milwaukee Public Museum by wrapping them in cheesecloth saturated with 70% EtOH; these cheesecloth bundles were then placed in three layers of plastic bagging and absorbent pads. Upon reaching the museum, the fishes were processed through a dehydration series, spending 24 to 72 hours in 10%, 35%, and 50% EtOH before being permanently stored in 70% EtOH. All institutional abbreviations follow Sabaj (2020).

Descriptions of external morphology follow Barel et al. (1977). External counts and measurements follow Barel et al. (1977), Stauffer et al. (1997), and Pauers (2016). Standard length (SL) is used throughout. Except for the counts of gill rakers, all counts and measurements were made on the left side of the fish. We also note that, contrary to Ahl's (1927) description, all the oral teeth in *Labeotropheus* are tricuspid, and most of the scales are ctenoid, except in the belly and anterior abdomen, where they are cycloid.

All measurements were taken to the nearest hundredth mm using digital calipers, and then rounded to the nearest one-tenth mm. Measurements taken on the trunk were standardized by SL, while those on the head were standardized by head length (HL). The morphometric and meristic data for *Labeotropheus fuelleborni* and *L. trewavasae*, the exemplar species for the robust and slender *Labeotropheus*, respectively, were measured by the lead author and are included for comparison in Table 2. The morphometric and meristic data from the three more recently described *Labeotropheus*, *L. chlorosiglos*, *L. simoneae*, and *L. artatorostris*, were measured by the lead author and can be found in Pauers (2016; *L. chlorosiglos* and *L. simoneae*) and Pauers (2017; *L. artatorostris*).

In order to diagnose putative new species of *Labeotropheus*, we followed Pauers (2016). Briefly, by first using the Evolutionary Species Concept (Simpson, 1961; Wiley, 1978) as a non-operational guiding principle (Mayden, 1999), the application of operational criteria were then used to distinguish one species from another.

**Analyses.**—Since many of the morphometric and meristic characteristics overlapped among species, we used canonical discriminant function analyses to assist the diagnoses of these species. We performed separate analyses on the Log<sub>10</sub>-transformed morphometric data and non-transformed meristic data. Comparisons among species were then illustrated by plotting pairs of morphometric and meristic canonical functions. The analyses were performed and function plots made in Systat 10.0.

***Labeotropheus alticodia*, Phiri and Pauers, new species**

urn:lsid:zoobank.org:act:1FF94795-F35C-4E43-B4EB-

5A04F906A3B3

Figures 2–4; Tables 3–5

**Holotype.**—SAIAB 211372, adult male, 78.2 mm SL, Malaŵi, Lake Malaŵi, Maleri Island, -13.9089591, 34.6260792, Michael J. Pauers, Titus B. Phiri, and Sanudi Likupe, 16 January 2020.

**Paratypes.**—FMNH 145009, 1 male, 79.4 mm SL, 1 female, 85.5 mm SL, Malaŵi, Lake Malaŵi, male: Maleri Island, -13.9089591, 34.6260792, female: Nankoma Island, -13.8840189, 34.6118803, Michael J. Pauers, Titus B. Phiri, and Sanudi Likupe, 16 January 2020; MPM Fi50085, 1 male, 77.1 mm SL, Malaŵi, Lake Malaŵi, Maleri Island, -13.9089591, 34.6260792, Michael J. Pauers, Titus B. Phiri, and Sanudi Likupe, 16 January 2020; MPM Fi50087, 1 female, 63.0 mm SL, Malaŵi, Lake Malaŵi, Maleri Island, -13.8926036, 34.6221075, Michael J. Pauers, Titus B. Phiri, and Sanudi Likupe, 16 January 2020; SAIAB 211373, 2 females, 79.4 and 85.1 mm SL, Malaŵi, Lake Malaŵi, Nankoma Island, -13.8840189, 34.6118803, Michael J. Pauers, Titus B. Phiri, and Sanudi Likupe, 16 January 2020.

**Diagnosis.**—*Labeotropheus alticodia* differs from the slender-bodied *Labeotropheus*, *L. trewavasae*, *L. simoneae*, *L. chirangali*, new species, and *L. rubidorsalis*, new species, as well as *L. chlorosiglos*, due to its greater body depth (37.4–40.6% SL vs. 26.3–33.4% SL in *L. trewavasae*; 26.9–30.8% SL in *L. simoneae*; 26.6–33.2% SL in *L. chirangali*, new species; 31.6–36.1% SL in *L. rubidorsalis*, new species; 31.9–34.7% SL in *L. chlorosiglos*). It also differs from the slender *Labeotropheus* due to a greater distance between the insertion of the dorsal fin and the insertion of the anal fin (16.4–18.1% SL vs. 12.7–15.5% SL in *L. trewavasae*; 14.6–16.0% SL in *L. simoneae*; 13.7–15.7% SL in *L. chirangali*, new species; 13.5–15.7% SL in *L. rubidorsalis*, new species). *Labeotropheus alticodia* differs from all other robust-bodied *Labeotropheus*, except *L. fuelleborni*, by the nuptial coloration of the males. Male *L. alticodia* have a pale, powder-blue body, and the dorsal and caudal fins are whitish blue with yellow trailing edges, while the anal fin is a pale yellow orange; additionally, the pelvic fins are a pale yellow orange with white leading edges. The morphometric and meristic values largely overlap with the other robust *Labeotropheus*, with the following exceptions: *L. alticodia*

**Table 2.** Morphometric and meristic values for *Labeotropheus fuelleborni* and *L. trewavasae*, the exemplar species for robust and slender *Labeotropheus*, respectively.

| (A) Morphometric data  | <i>Labeotropheus fuelleborni</i> (n = 5) |           |             | <i>L. trewavasae</i> (n = 12) |          |           |
|--|--|-----------|-------------|-------------------------------|----------|-----------|
|  | Lectotype                                | Mean±SE   | Range       | Holotype                      | Mean±SE  | Range     |
| Standard length (SL, mm)                                     | 91.7                                     | 90.1±6.3  | 67.1–101.7  | 79.4                          | 81.3±2.0 | 63.1–89.3 |
| Head length (HL, mm)   | 29.4                                     | 27.9±1.9  | 20.8–31.8   | 24.7                          | 24.8±0.6 | 19.1–26.8 |
| % SL   |  |           |             |                               |          |           |
| HL   | 32.0                                     | 30.9±0.6  | 28.9–32.0   | 31.1                          | 30.6±0.3 | 28.7–32.3 |
| Snout to origin of dorsal fin (DFO)                          | 33.2                                     | 32.8±0.5  | 30.8–33.8   | 34.5                          | 32.5±0.5 | 30.1–35.8 |
| Snout to attachment of pelvic fins (PFO)                     | 39.7                                     | 41.3±1.0  | 39.5–44.6   | 35.5                          | 37.1±0.6 | 33.7–41.3 |
| Length of pectoral fin                                       | 24.4                                     | 24.3±0.5  | 23.2–25.7   | 22.5                          | 22.2±0.2 | 20.8–23.9 |
| DFO to origin of anal fin (AFO)                              | 53.2                                     | 53.6±0.6  | 52.5–55.5   | 47.6                          | 49.0±0.4 | 46.7–51.6 |
| Insertion of dorsal fin (DFI) to insertion of anal fin (AFI) | 17.0                                     | 16.9±0.2  | 16.5–17.4   | 13.8                          | 13.8±0.2 | 12.7–15.5 |
| DFO to AFI   | 64.3                                     | 62.0±1.8  | 55.1–65.0   | 62.3                          | 61.2±0.9 | 51.8–64.3 |
| DFI to AFO   | 31.6                                     | 30.8±0.4  | 29.6–31.7   | 26.6                          | 27.3±0.3 | 26.3–29.1 |
| DFI to ventral attachment of caudal fin                      | 19.0                                     | 19.0±0.1  | 18.7–19.3   | 18.0                          | 16.9±0.3 | 15.4–18.2 |
| AFI to dorsal attachment of caudal fin                       | 20.9                                     | 20.2±0.3  | 19.6–20.9   | 20.2                          | 18.6±0.3 | 16.7–20.2 |
| DFO to attachment of pelvic fins                             | 38.0                                     | 37.6±1.2  | 34.9–41.7   | 28.0                          | 29.8±0.6 | 27.1–32.7 |
| DFI to attachment of pelvic fins                             | 56.5                                     | 55.9±0.5  | 54.1–57.2   | 53.5                          | 54.9±0.6 | 52.5–57.9 |
| Body depth   | 37.5                                     | 37.3±1.2  | 35.2–41.6   | 27.8                          | 29.5±0.6 | 26.3–33.4 |
| Width at opercular tabs                                      | 16.5                                     | 16.8±0.4  | 16.2–18.2   | 15.1                          | 15.6±0.3 | 13.4–17.2 |
| Width at pectoral fins                                       | 15.6                                     | 16.0±0.3  | 15.0–16.9   | 13.6                          | 14.5±0.4 | 12.1–16.6 |
| Width at pelvic fins   | 8.2                                      | 8.1±0.2   | 7.5–8.5     | 7.1                           | 7.1±0.1  | 6.8–7.6   |
| % HL   |  |           |             |                               |          |           |
| Eye diameter   | 25.0                                     | 25.3±0.5  | 23.7–26.6   | 23.4                          | 25.0±0.4 | 23.2–27.7 |
| Preorbital depth   | 28.8                                     | 27.5±0.8  | 25.2–29.6   | 24.9                          | 25.0±0.6 | 21.2–27.6 |
| Cheek depth  | 26.6                                     | 27.7±1.3  | 23.7–30.8   | 22.0                          | 23.2±0.7 | 19.7–27.2 |
| Snout length   | 31.4                                     | 29.8±0.8  | 27.2–31.4   | 28.3                          | 28.7±0.6 | 24.5–33.2 |
| Rostral length   | 42.0                                     | 41.2±0.4  | 40.4–42.1   | 38.5                          | 38.3±0.8 | 35.3–45.8 |
| Upper jaw length (UJL)                                       | 21.0                                     | 21.5±0.6  | 20.2–23.9   | 19.4                          | 18.9±0.5 | 16.7–21.3 |
| Snout pad length   | 15.2                                     | 16.1±0.4  | 14.9–17.2   | 9.1                           | 12.4±0.5 | 9.1–14.7  |
| Lower jaw length (LJL)                                       | 28.3                                     | 30.4±1.8  | 28.0–37.4   | 29.0                          | 28.9±1.0 | 23.0–33.3 |
| Lower jaw width (LJW)  | 45.3                                     | 50.4±1.6  | 45.3–53.9   | 38.3                          | 40.0±0.9 | 34.7–43.9 |
| Head depth   | 101.3                                    | 105.8±2.4 | 101.2–113.4 | 84.9                          | 89.1±1.7 | 80.1–99.1 |
| Interorbital width   | 36.0                                     | 39.2±1.3  | 36.0–42.8   | 31.6                          | 34.0±1.0 | 29.7–40.5 |
| Snout width  | 38.2                                     | 41.0±0.9  | 38.2–43.9   | 34.1                          | 35.2±0.6 | 31.5–37.9 |
| (B) Meristic data  | Lectotype                                | Mode      | Range       | Holotype                      | Mode     | Range     |
| Anterior lateral line scales (LLS)                           | 22                                       | 22        | 21–22       | 24                            | 24       | 22–27     |
| Posterior LLS  | 13                                       | 13        | 11–14       | 14                            | 12       | 10–14     |
| Overlapping LLS  | 1  | 1         | 0–3         | 5                             | 4        | 0–5       |
| Dorso-lateral scale rows                                     | 9  | 9         | 9–10        | 8                             | 9        | 7–10      |
| Pectoro-pelvic scale rows                                    | 10                                       | 10        | 9–12        | 12                            | 12       | 7–12      |
| Cheek scale rows   | 4  | 3         | 3–4         | 3                             | 4        | 3–5       |
| Dorsal-fin spines (DFS)                                      | 17                                       | 17        | –           | 18                            | 19       | 18–19     |
| Dorsal-fin rays (DFR)  | 8  | 9         | 8–9         | 9                             | 8        | 8–9       |
| Anal-fin spines (AFS)  | 3  | 3         | –           | 3                             | 3        | –         |
| Anal-fin rays (AFR)  | 7  | 7         | 6–7         | 7                             | 7        | 7–9       |
| Pectoral-fin rays  | 14                                       | 14        | –           | 13                            | 13       | 12–14     |
| Pelvic-fin rays  | 6  | 6         | –           | 6                             | 6        | –         |
| Upper jaw teeth rows   | 5  | 5         | 4–5         | 5                             | 5        | 5–7       |
| Lower jaw teeth rows   | 6  | 6         | –           | 6                             | 6        | 5–6       |
| Teeth on left lower jaw                                      | 42                                       | 40        | 31–43       | 26                            | 27       | 25–34     |
| Teeth on left dentigerous premaxilla                         | 8  | 8         | 6–9         | 6                             | 7        | 4–10      |
| Total gill rakers  | 11                                       | 11        | 10–11       | 13                            | 12       | 9–13      |
| Epibranchial gill rakers                                     | 2  | 2         | 2–3         | 3                             | 2        | 2–3       |
| Ceratobranchial gill rakers                                  | 8  | 7         | 7–8         | 9                             | 9        | 6–9       |
| Infraorbital pores   | 9  | 9         | –           | 9                             | 9        | 7–9       |
| Neuromasts within infraorbital pores                         | 32                                       | 27        | 22–40       | 20                            | 20       | 8–25      |



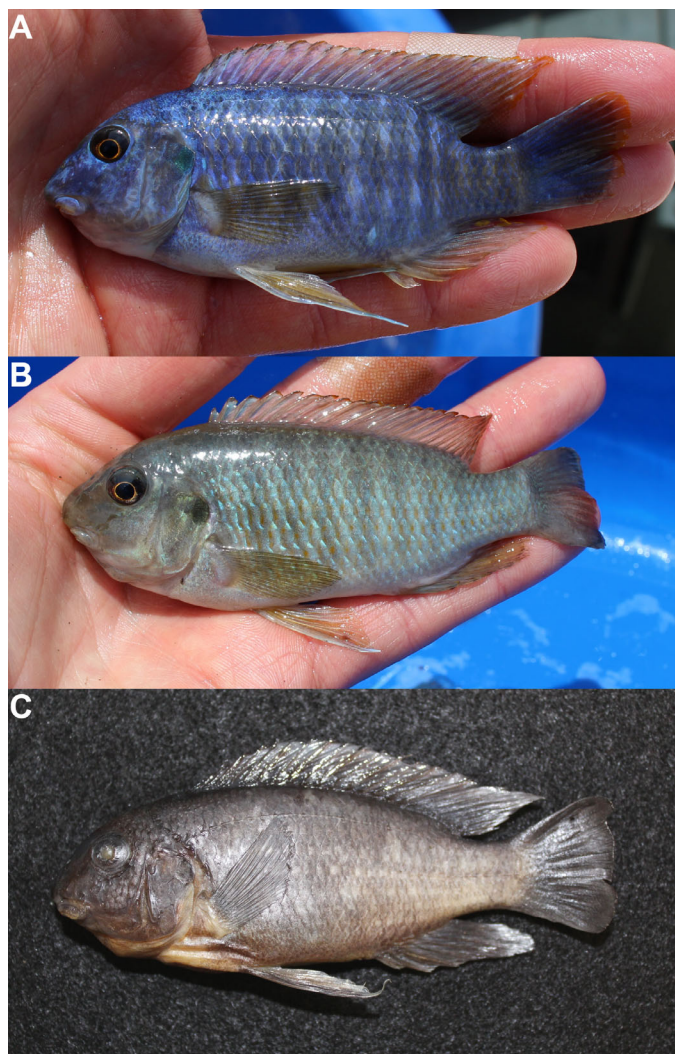


**Fig. 2.** *Labeotropheus alticodia*, new species. (A) Live male holotype (SAIAB 211372), 78.2 mm SL; (B) live female paratype (SAIAB 211373), 85.1 mm SL; (C) holotype after preservation.

differs from *L. fuelleborni* due to a longer distance between the tip of the snout and the origin of the dorsal fin (33.6–35.9% SL vs. 30.8–33.7%), a longer rostral length (42.0–48.4% HL vs. 40.4–42.0%), a shorter upper jaw (14.4–20.1% HL vs. 20.2–23.9%), and a smaller snout pad (11.6–14.8% HL vs. 14.9–17.2%). *Labeotropheus alticodia* differs from *L. artatorostris* due to a deeper preorbital depth (26.9–34.5% HL vs. 19.7–26.8%) and a typically longer rostral length (42.0–48.4% HL vs. 22.9–43.7%). It differs from *L. candipygia*, new species, by greater distances between the insertion of the dorsal fin and the insertion of the anal fin (16.4–18.1% SL vs. 13.9–16.7%) as well as between the insertion of the dorsal fin and the origin of the anal fin (31.3–32.9% SL vs. 27.4–31.7%). *Labeotropheus alticodia* differs from *L. aurantinfra*, new species, by a greater distance between the tip of the snout and the attachment of the pelvic fins (41.0–49.1% SL vs. 36.9–43.7%), a greater preorbital depth (26.9–34.5% HL vs. 21.3–31.7%), and a greater snout length (30.4–35.7% HL vs. 26.7–33.1%). Finally, *L. alticodia* differs from *L. obscurus*, new species, due to a smaller eye diameter (24.9–27.5% HL vs. 27.3–32.4%) and more teeth in the left half of the lower jaw (29–35 vs. 20–26).

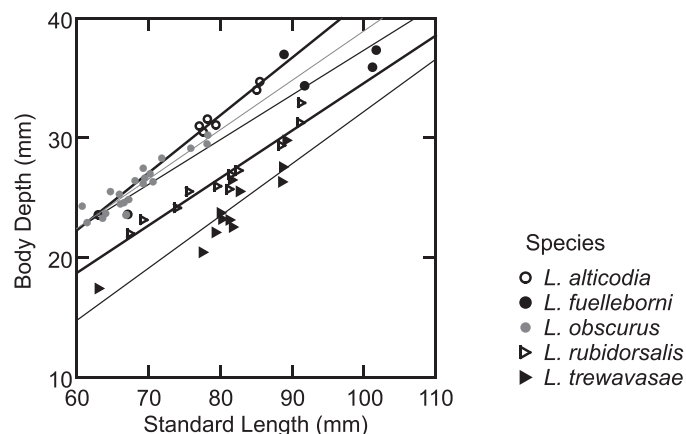


**Fig. 3.** Body depth–standard length relationships among *L. fuelleborni*, *L. trewavasae*, and the three new species of *Labeotropheus* from the southwestern portion of Lake Malaŵi. The ANOVA accompanying these data is in Table 4.

**Description.**—Morphometric and meristic data summarized in Table 3. Body compressiform; ovoid to almost rectangular in shape. Body deep (37.4–40.6% SL) and consistently deep throughout its length. Anterior body wide at pectoral fin and opercular tab. Scales on belly and anterior abdomen cycloid and tightly crowded. Flank scales ctenoid; exposed portion of scale fan-shaped and approximately hexagonal. Anterior lateral line overlapping posterior lateral line by 0–4 scales. Dorsal fin relatively short for *Labeotropheus* (55.8–60.2% SL) with 16–17 spines and 8–9 rays. First dorsal spine opposite opercular tab. Dorsal rays 3, 4, 5 long, reaching to hypural plate and beyond. Anal fin angular and kite-shaped; anal-fin rays 3 and 4 long, reaching past caudal peduncle to caudal fin. Anal-fin origin opposite dorsal-fin spine 14 or 15; anal-fin insertion anterior to dorsal-fin insertion. Caudal fin subtruncate. Pectoral fin rounded. Pelvic fin long, minimally reaching origin of anal fin and longer in most specimens; males with filamentous pelvic rays, females non-filamentous. Attachment of pelvic fin opposite dorsal-fin spine 5 or 6.

Head of typical length for *Labeotropheus* (31.8–33.4% SL) but deep with strongly curved profile and slightly developed snout. Snout long and wide with snout pad of typical length for *Labeotropheus* (11.6–14.8% HL). Cheek with 3 scale rows. Infraorbital pores 9, with 23–38 neuromasts among them. Oral jaws short and wide. Oral teeth tricuspid and closely set on both upper and lower jaws; 7–10 tricuspid teeth on lateral portion of left upper jaw. Gill rakers stout, triangular, and widely spaced; 6–8 ceratobranchial and 2–3 epibranchial gill rakers on first gill arch. All specimens with 1 raker between the cerato- and epibranchial rakers.

**Coloration of males.**—Craniofacial region, from snout to preopercle, dark blue. Operculum grayish blue with bright metallic green opercular tab. Throat and branchiostegals white. Flank and caudal peduncle pale powder blue; 11 faint darker blue bars visible across flank and caudal peduncle. Dorsal and caudal fins whitish blue with yellow or orange trailing edges. Spinous anal fin pale orange; rayed portion white with 3–5 orange-yellow eggspots. Trailing portion of pelvic fin hyaline with white leading edge, and pale orange between.

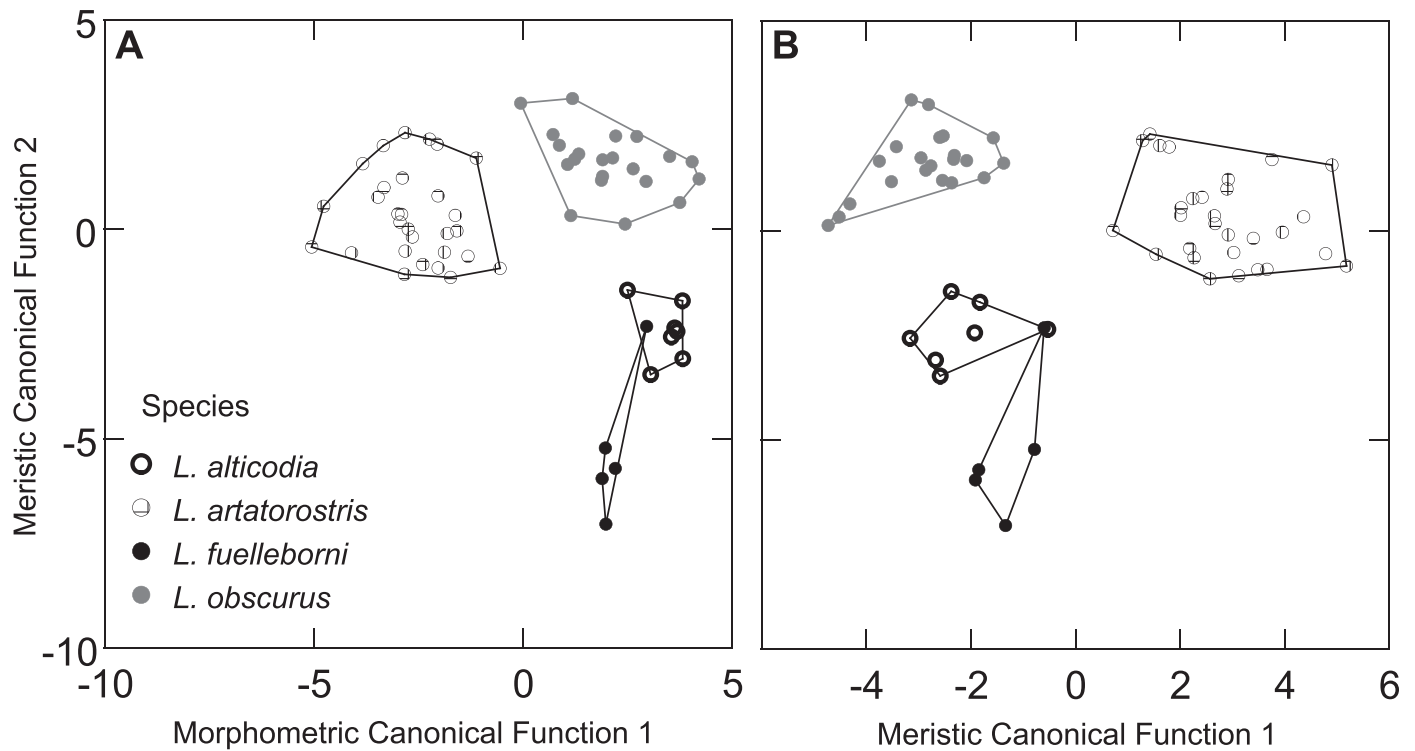


**Fig. 4.** Canonical function plots for robust *Labeotropheus* from the southwestern portion of Lake Malaŵi. (A) Morphometric canonical function 1 vs. meristic function 2; (B) meristic canonical function 1 vs. meristic function 2.

In preservative, males uniformly dark brown or gray with 11 faint vertical bars visible across flank and caudal peduncle on some specimens.

**Coloration of females.**—Head, body, caudal peduncle uniformly light gray, with 11 faint dark bars extending across flank and caudal peduncle. Opercular tab black. Scales of flank and caudal peduncle with small orange spots close to insertion of scale. Throat and branchiostegals white. Dorsal fin white with orange tips; some specimens with orange spots throughout fin, some specimens with orange trailing edge. Caudal fin brownish gray, some specimens with orange trailing edge. Rayed anal fin pale brownish orange with 1–2 yellow eggspots; spinous portion white. Pelvic fin white or hyaline, with bright white leading edge and pale orange between.

In preservative, females uniformly dark brown or gray with 11 faint vertical bars visible across flank and caudal peduncle on some specimens.

**Multivariate analyses.**—Due to the overlap of morphometric and meristic characteristics between *L. alticodia* and the other *Labeotropheus*, we compared the body depth–standard length ratios of *L. alticodia* and its geographically proximate congeners (Fig. 3). This ratio clearly places *L. alticodia* with the robust *Labeotropheus*, and distinguishes it from *L. trewasae* and the sympatric *L. rubidorsalis*, new species (Table 4). We also performed canonical discriminant function analyses on the meristic and  $\text{Log}_{10}$ -transformed morphometric data. Both the morphometric and meristic canonical discriminant function analyses were robust and produced statistically significant results (Table 5). *Labeotropheus alticodia* is distinct from *L. artatorostris* and *L. obscurus*, new species, along the first morphometric canonical function and

the first two meristic canonical functions, although there is minor overlap with *L. fueelleborni* (Fig. 4).

**Distribution.**—*Labeotropheus alticodia* is endemic to Lake Malaŵi and appears to be restricted to the Maleri Islands, specifically Maleri and Nankoma Islands, in Lake Malaŵi National Park, Malaŵi. We did not collect at the nearby Nakantenga Island, where Ribbink et al. (1983a) report a differently colored robust *Labeotropheus*.

**Etymology.**—The specific epithet combines the Latin adjective for deep or tall, *alti*, with a Latin word for head, specifically the head of a flower, *codia*, in reference to the striking head depth of this species.

***Labeotropheus aurantinfra*, Phiri and Pauers, new species**

urn:lsid:zoobank.org:act:68D4FDCB-80DF-44E2-977A-A7A7678CE748

Figures 5–7; Tables 6–9

**Holotype.**—SAIAB 211375, adult male, 114.8 mm SL, Malaŵi, Lake Malaŵi, Chirwa Island, –10.4684007, 34.2811572, Michael J. Pauers, Titus B. Phiri, Victor Nantunga, and Stuart M. Grant, Ltd, crew, 1 August 2018.

**Paratypes.**—FMNH 145010, 1 male, 98.4 mm SL, 1 female, 90.8 mm SL, Africa, Lake Malaŵi, Chirwa Island, –10.4684007, 34.2811572, Michael J. Pauers, Titus B. Phiri, Victor Nantunga, and Stuart M. Grant, Ltd, crew, 1 August 2018; MPM Fi50071, 12 males, 9 females, 72.9–111.7 mm SL, Malaŵi, Lake Malaŵi, Chirwa Island, –10.4684007, 34.2811572, Michael J. Pauers, Titus B. Phiri, Victor Nantunga, and Stuart M. Grant, Ltd, crew, 1 August 2018; MPM 50077, 5 males, 10 females, 64.8–107.5 mm SL, Malaŵi, Lake Malaŵi, Ndomo Gap, –10.4350479,

**Table 3.** Morphometric and meristic values for *Labeotropheus alticodia*, new species ( $n = 7$ ).

| (A) Morphometric data  | Holotype | Mean $\pm$ SE   | Range      |
|--|----------|-----------------|------------|
| Standard length (SL, mm)                                     | 78.2     | 78.0 $\pm$ 2.8  | 63.0–85.5  |
| Head length (HL, mm)   | 24.9     | 25.5 $\pm$ 1.0  | 20.2–28.5  |
| % SL   |          |                 |            |
| HL   | 31.9     | 32.6 $\pm$ 0.2  | 31.9–33.4  |
| Snout to origin of dorsal fin (DFO)                          | 35.9     | 35.0 $\pm$ 0.3  | 33.6–35.9  |
| Snout to attachment of pelvic fins (PFO)                     | 43.7     | 45.3 $\pm$ 1.1  | 41.0–49.1  |
| Length of pectoral fin                                       | 23.5     | 24.9 $\pm$ 0.7  | 22.5–28.4  |
| Length of base of dorsal fin                                 | 60.3     | 58.0 $\pm$ 0.6  | 55.8–60.3  |
| DFO to origin of anal fin (AFO)                              | 53.5     | 52.8 $\pm$ 0.2  | 52.2–53.5  |
| Insertion of dorsal fin (DFI) to insertion of anal fin (AFI) | 16.8     | 17.1 $\pm$ 0.2  | 16.4–18.1  |
| DFO to AFI   | 63.5     | 62.2 $\pm$ 0.4  | 60.4–63.5  |
| DFI to AFO   | 32.4     | 31.8 $\pm$ 0.2  | 31.3–32.9  |
| DFI to ventral attachment of caudal fin                      | 20.2     | 19.5 $\pm$ 0.4  | 18.0–21.2  |
| AFI to dorsal attachment of caudal fin                       | 21.5     | 21.1 $\pm$ 0.4  | 20.2–23.2  |
| DFO to attachment of pelvic fins                             | 38.7     | 39.4 $\pm$ 0.5  | 36.8–40.6  |
| DFI to attachment of pelvic fins                             | 54.4     | 54.2 $\pm$ 0.4  | 52.9–56.2  |
| Body depth   | 40.4     | 39.6 $\pm$ 0.4  | 37.4–40.6  |
| Width at opercular tabs                                      | 16.4     | 17.6 $\pm$ 0.4  | 16.4–19.4  |
| Width at pectoral fins                                       | 15.8     | 16.7 $\pm$ 0.7  | 13.2–18.9  |
| Width at pelvic fins   | 7.7      | 8.2 $\pm$ 0.1   | 7.7–8.8    |
| % HL   |          |                 |            |
| Eye diameter   | 26.4     | 26.3 $\pm$ 0.3  | 24.9–27.5  |
| Preorbital depth   | 26.9     | 31.4 $\pm$ 1.1  | 26.9–34.5  |
| Cheek depth  | 31.0     | 30.0 $\pm$ 0.9  | 25.9–32.5  |
| Snout length   | 30.4     | 33.3 $\pm$ 0.8  | 30.4–35.7  |
| Rostral length   | 43.0     | 45.0 $\pm$ 0.9  | 42.0–48.4  |
| Upper jaw length (UJL)                                       | 20.0     | 18.7 $\pm$ 0.8  | 14.4–20.2  |
| Snout pad length   | 14.1     | 13.0 $\pm$ 0.4  | 11.6–14.8  |
| Lower jaw length (LJL)                                       | 36.0     | 33.3 $\pm$ 1.3  | 27.4–36.4  |
| Lower jaw width (LJW)  | 47.7     | 44.1 $\pm$ 0.8  | 41.4–47.7  |
| Head depth   | 108.3    | 108.1 $\pm$ 1.6 | 99.1–111.4 |
| Interorbital width   | 36.8     | 37.8 $\pm$ 0.7  | 34.6–40.3  |
| Snout width  | 40.9     | 38.6 $\pm$ 0.8  | 34.9–41.1  |
| (B) Meristic data  | Holotype | Mode            | Range      |
| Anterior lateral line scales (LLS)                           | 23       | 22              | 21–24      |
| Posterior LLS  | 12       | 12              | 11–13      |
| Overlapping LLS  | 1        | 1               | 0–4        |
| Dorso-lateral scale rows                                     | 9        | 9               | 9–10       |
| Pectoro-pelvic scale rows                                    | 11       | 10              | 10–12      |
| Cheek scale rows   | 3        | 3               | –          |
| Dorsal-fin spines (DFS)                                      | 17       | 17              | 16–17      |
| Dorsal-fin rays (DFR)  | 8        | 8               | 8–9        |
| Anal-fin spines (AFS)  | 3        | 3               | –          |
| Anal-fin rays (AFR)  | 7        | 7               | 7–8        |
| Anal-fin spines (AFS)  | 3        | 3               | –          |
| Anal-fin rays (AFR)  | 7        | 7               | 7–8        |
| Pectoral-fin rays  | 14       | 14              | 13–16      |
| Pelvic-fin rays  | 6        | 6               | –          |
| Upper jaw teeth rows   | 4        | 4               | 3–5        |
| Lower jaw teeth rows   | 4        | 5               | 4–5        |
| Teeth on left lower jaw                                      | 33       | 34              | 29–35      |
| Teeth on left dentigerous premaxilla                         | 8        | 10              | 7–10       |
| Total gill rakers  | 10       | 11              | 10–12      |
| Epibranchial gill rakers                                     | 3        | 2               | 2–3        |
| Ceratobranchial gill rakers                                  | 6        | 8               | 6–8        |
| Infraorbital pores   | 9        | 9               | –          |
| Neuromasts within infraorbital pores                         | 30       | 32              | 23–38      |



**Table 4.** Analysis of variance on body depth vs. standard length for southwestern *Labeotropheus*.**(A) Analysis of variance ( $n = 56$ ; multiple  $R^2 = 0.933$ )**

| Variable                  | Sum of squares | df | Mean square | F       | P            |
|---------------------------|----------------|----|-------------|---------|--------------|
| Species                   | 6.385          | 4  | 1.596       | 1.106   | 0.365        |
| Standard length           | 446.940        | 1  | 446.940     | 309.574 | $\leq 0.001$ |
| Species * standard length | 3.208          | 4  | 0.802       | 0.556   | 0.696        |
| Error                     | 66.411         | 46 | 1.444       |         |              |

**(B) Pairwise comparisons: \*  $P \leq 0.001$ ; <sup>ns</sup> = not significant**

|                        | <i>L. alticodia</i>  | <i>L. fuelleborni</i> | <i>L. obscurus</i> | <i>L. rubidorsalis</i> |
|------------------------|----------------------|-----------------------|--------------------|------------------------|
| <i>L. fuelleborni</i>  | -1.676 <sup>ns</sup> |                       |                    |                        |
| <i>L. obscurus</i>     | -0.979 <sup>ns</sup> | 0.698 <sup>ns</sup>   |                    |                        |
| <i>L. rubidorsalis</i> | -4.954*              | -3.278*               | -3.976*            |                        |
| <i>L. trewavasae</i>   | -8.262*              | -6.585*               | -7.283*            | -3.307*                |

34.2643444, Michael J. Pauers, Titus B. Phiri, Victor Nantunga, and Shaibu Fisha, 2 August 2018; SAIAB 211374, 1 male, 90.6 mm SL, 2 females, 88.8 and 98.1 mm SL, Malaŵi, Lake Malaŵi, Chirwa Island, -10.4684007, 34.2811572, Michael J. Pauers, Titus B. Phiri, Victor Nantunga, and Stuart M. Grant, Ltd, crew, 1 August 2018.

**Diagnosis.**—*Labeotropheus aurantinfra* differs from all other *Labeotropheus* due to the extensive distribution of orange pigmentation throughout the body, including the maxilla, the preopercular margin, the branchiostegals, the gular and anterior abdomen region, and the flanks; although orange pigmentation is more common and more extensive in males, it is also present in the same body regions in females. *Labeotropheus aurantinfra* differs from the slender-bodied *Labeotropheus*, *L. trewavasae*, *L. simoneae*, *L. chirangali*, new species, but not *L. rubidorsalis*, new species, due to its greater body depth (33.8–41.5% SL vs. 26.3–33.4% in *L. trewavasae*; 26.9–30.8% in *L. simoneae*; and 26.6–33.2% in *L. chirangali*, new species). While *L. aurantinfra* does have a deeper body than *L. rubidorsalis*, new species, the ranges overlap (33.8–41.5% SL vs. 31.6–36.1%). *Labeotropheus aurantinfra* has a greater distance between the origin of the dorsal fin and the attachment of the pelvic fins (33.4–40.4% SL vs. 31.5–35.4%), a shorter lower jaw (22.5–31.6% HL vs. 29.9–38.5%), more rows of teeth in the upper jaw (4–6 vs. 3–4), and a greater total number of gillrakers (10–15 vs. 9–11) than *L. rubidorsalis*, new species.

This primary distinction between *L. aurantinfra* and the other robust-bodied *Labeotropheus* is the unique distribution of yellow-orange pigmentation across the body, especially in the males. The morphometric and meristic values largely overlap with the other robust *Labeotropheus*, although there are some distinctions, including those noted for *L. alticodia* above. *Labeotropheus aurantinfra* has a typically greater distance between the tip of the snout and the origin of the dorsal fin than *L. fuelleborni* (31.8–37.4% SL vs. 30.7–33.8%), a typically greater distance between the origin of the dorsal fin and the insertion of the anal fin than *L. fuelleborni* (60.8–69.5% SL vs. 55.1–64.9%), and typically more anal-fin rays than *L. fuelleborni* (7–9 vs. 6–7). Compared to *L. chlorosiglos*, *L. aurantinfra* has a greater eye diameter (23.5–32.4% HL vs. 22.6–25.5%), a longer rostral length (36.1–51.1% HL vs. 34.7–41.1%), a greater pectoral width (13.2–18.9% SL vs. 12.7–14.3%), and a greater number of scale rows between the pectoral and pelvic fins (9–12 vs. 6–9). *Labeotropheus aurantinfra*

*fra* differs from *L. artatorostris* due to its greater rostral length (36.1–51.1% HL vs. 22.9–43.7%), a larger snout pad (10.5–19.4% HL vs. 7.4–16.1%), and more infraorbital neuromasts (25–40 vs. 12–36). *Labeotropheus aurantinfra* differs from *L. obscurus*, new species, due to a typically shorter lower jaw (22.5–31.6% HL vs. 27.6–40.4%), a greater number of rows of teeth in the upper jaw (4–6 vs. 3–4), and a greater number of teeth in the left half of the lower jaw (24–37 vs. 20–26). This species differs from *L. candipygia*, new species, due to a greater distance between the origin of the dorsal fin and the insertion of the anal fin (60.7–69.6% SL vs. 50.6–66.8%), and a greater head depth (86.0–116.6% HL vs. 87.9–108.1%).

**Description.**—Morphometric and meristic data summarized in Table 6. Compressiform body with expanded ovoid shape; depth typical for a robust *Labeotropheus* (33.8–41.5% SL), and body consistently deep throughout its length. Body wide at pectoral fin and opercular tabs. Scales on belly and anterior abdomen cycloid and tightly crowded. Flank scales ctenoid; exposed portion of scale fan-shaped and approximately hexagonal. Anterior lateral line overlapping posterior lateral line by 0–3 scales. Dorsal fin long (56.3–62.9% SL); 17–19 spines and 7–9 rays. First dorsal spine anterior to or opposite opercular tab. Dorsal rays 3, 4, 5 long, reaching to hypural and beyond. Anal fin angular and kite-shaped. Anal rays 3, 4, 5 long in males, reaching past caudal peduncle to caudal fin; most female specimens with short anal-fin rays, reaching only to caudal peduncle. Anal-fin origin opposite dorsal-fin spine 14, 15, or 16; anal-fin insertion anterior to or opposite dorsal-fin insertion. Caudal fin subtruncate. Pectoral fin long and rounded, 12–14 rays. Pelvic fin long, minimally reaching origin of anal fin and longer in most specimens, especially in mature males; pelvic ray slightly produced and filamentous in all specimens. Pelvic-fin attachment opposite dorsal-fin spine 5 or 6.

Head short (29.1–38.8% SL) and deep with strongly curved profile and prominent snout; some specimens with concavity above eye. Snout long and wide, typical of *Labeotropheus*, with long snout pad (10.5–19.4% HL). Cheek deep with 3–4 scale rows. Infraorbital pores 8–10 with 15–67 neuromasts among them. Oral jaws short and wide. Oral teeth tricuspid and closely set on both upper and lower; 5–11 tricuspid teeth on lateral portion of left upper jaw. Gill rakers stout, triangular, and widely spaced; 7–10 ceratobranchial and 1–3 epibranchial gill rakers on first gill arch. All specimens with 1 raker between the cerato- and epibranchial rakers.

**Table 5.** Canonical discriminant function (CDF) analyses on (A)  $\text{Log}_{10}$ -transformed morphometric and (B) meristic data for *L. artatorostris*, *L. alticodia*, *L. fuelleborni*, and *L. obscurus*. Standardized functions are reported. Uninformative variables are omitted.

(A)  $\text{Log}_{10}$ -transformed morphometric data: Wilks'  $\lambda = 0.019$ ,  $F_{30,147} = 13.904$ ,  $P \leq 0.001$

|                         | CDF 1  | CDF 2  | CDF 3  |
|-------------------------|--------|--------|--------|
| Eigenvalue              | 6.849  | 2.616  | 0.813  |
| Canonical correlation   | 0.934  | 0.851  | 0.670  |
| SL                      | 0.866  | 0.912  | 5.641  |
| HL                      | -3.881 | -1.153 | -2.397 |
| Width at opercular tabs | -3.081 | -3.349 | -1.518 |
| Width at pectoral fins  | 1.035  | 2.222  | 0.123  |
| Preorbital depth        | 1.132  | 0.460  | -1.452 |
| Cheek depth             | 1.833  | -0.933 | -0.155 |
| Rostral length          | 1.560  | 0.159  | -0.157 |
| Snout pad length        | 0.796  | 0.616  | 0.422  |
| Lower jaw length (LJL)  | -0.356 | -1.555 | -0.385 |
| Lower jaw width (LJW)   | 0.445  | 2.982  | -0.519 |
| Species means           |        |        |        |
| <i>L. alticodia</i>     | 3.430  | 0.554  | -2.145 |
| <i>L. artatorostris</i> | -2.624 | 0.056  | -0.139 |
| <i>L. fuelleborni</i>   | 2.198  | 4.723  | 1.152  |
| <i>L. obscurus</i>      | 2.082  | -1.390 | 0.639  |

(B) Meristic data: Wilks'  $\lambda = 0.019$ ,  $F_{54,122} = 6.305$ ,  $P \leq 0.001$

|                                      | CDF 1  | CDF 2  | CDF 3  |
|--------------------------------------|--------|--------|--------|
| Eigenvalue                           | 7.655  | 4.093  | 0.182  |
| Canonical correlation                | 0.940  | 0.896  | 0.392  |
| Anterior lateral line scales (LLS)   | 0.102  | 0.300  | 0.169  |
| Posterior LLS                        | 0.018  | 0.144  | 0.167  |
| Overlapping LLS                      | 0.130  | 0.207  | -0.220 |
| Dorso-lateral scale rows             | -0.175 | -0.096 | 0.227  |
| Pectoro-pelvic scale rows            | -0.537 | -0.171 | 0.400  |
| Cheek scale rows                     | 0.245  | 0.131  | 0.583  |
| Dorsal-fin spines (DFS)              | 0.160  | 0.172  | 0.388  |
| Dorsal-fin rays (DFR)                | 0.276  | -0.140 | 0.296  |
| Anal-fin rays (AFR)                  | 0.024  | 0.177  | -0.342 |
| Pectoral-fin rays                    | -0.077 | -0.303 | 0.018  |
| Upper jaw teeth rows                 | 1.159  | 0.335  | -0.168 |
| Lower jaw teeth rows                 | -0.416 | -0.327 | 0.499  |
| Teeth on left lower jaw              | -0.016 | -1.100 | -0.119 |
| Teeth on left dentigerous premaxilla | 0.040  | 0.203  | -0.673 |
| Total gill rakers                    | 0.175  | 0.231  | 0.017  |
| Epibranchial gill rakers             | -0.193 | -0.494 | 0.042  |
| Infraorbital pores                   | -0.017 | -0.036 | 0.230  |
| Neuromasts within infraorbital pores | -0.521 | 0.255  | 0.015  |
| Species means                        |        |        |        |
| <i>L. alticodia</i>                  | -2.153 | -2.439 | -0.981 |
| <i>L. artatorostris</i>              | 2.819  | 0.324  | -0.009 |
| <i>L. fuelleborni</i>                | -1.296 | -5.251 | 0.821  |
| <i>L. obscurus</i>                   | -2.867 | 1.616  | 0.144  |

**Coloration of males.**—All males with orange pigmentation on maxilla, preopercular margin, branchiostegals, gular region, and anterior abdomen, extending across ventrum in most individuals. Opercular tab metallic blue-green or metallic green. Head, operculum, dorsum bright sky blue in most individuals, rarely a dull gray blue. Scales of flank and caudal peduncle sky blue or gray blue, ringed with orange; orange ring may be thin, with blue predominating, or may cover the

entire scale. In some individuals, orange may extend over entire body, including head, flank, and caudal peduncle; in these individuals, head and dorsum with brown or greenish sheen. 11 faint bars visible across flank and caudal peduncle. Dorsal fin predominantly bluish white; proximal portion of dorsal fin may have orange patches extending from dorsum. Trailing edge of dorsal fin orange. Caudal fin blue proximally, grading to black at the distal end; thin yellow trailing edge. Anal fin white or whitish gray with several (3–8) orange yellow eggspots. Pelvic fin pale red or orange with bright white leading edge; prominent black band separating leading edge from posterior color.

In preservative, males uniformly dark brown or gray with 11 faint vertical bars across the flank and caudal peduncle on some specimens. Some individuals with brown spots or rings on scales of flank and ventrum.

**Coloration of females.**—Head, body, and caudal peduncle uniformly light gray, with 11 faint dark bars extending across flank and caudal peduncle. Opercular tab black with metallic green sheen. Orange pigmentation on maxilla, preopercular margin, branchiostegals, gular region, and anterior abdomen, though not as prominent as on males. Scales of flank and caudal peduncle with small orange spots close to insertion of scale. Throat and branchiostegals white. Dorsal fin whitish gray. Caudal fin brownish gray. Anal fin whitish gray with 1–2 yellow eggspots. Pelvic fin white or hyaline, with bright white leading edge and pale orange between. One female *L. aurantinfra* had an orange blotch ('OB') color pattern across entire body and all fins; ground color is pale orange with black, white, and darker orange spots of varying shape and size.

In preservative, females uniformly dark brown or gray with 11 faint vertical bars visible across the flank and caudal peduncle on some specimens. 'OB' female appears pale gray with black and white spots across body and fins.

**Multivariate analyses.**—Due to the overlap of morphometric and meristic characteristics between *L. aurantinfra* and the other *Labeotropheus*, we compared the body depth–standard length ratios of *L. aurantinfra* and its geographically proximate congeners (Fig. 6). This ratio clearly places *L. alticodia* with the robust *Labeotropheus*, and distinguishes it from the slender *L. simoneae* and *L. chirangali*, new species, as well as the intermediate *L. chlorosiglos* (Table 7). We also performed canonical discriminant function analyses on the meristic and  $\text{Log}_{10}$ -transformed morphological data for *L. aurantinfra*, *L. candipygia*, new species, *L. chlorosiglos*, and *L. fuelleborni*. The canonical discriminant function analyses were robust and significant (Table 8). When the first morphometric canonical function is plotted against the first meristic canonical function, *L. chlorosiglos* is distinct along both axes, but there is some overlap among *L. aurantinfra*, *L. candipygia*, new species, and *L. fuelleborni* (Fig. 7A). Similarly, when the first two meristic canonical functions are plotted, *L. chlorosiglos* is distinct along meristic canonical function one, and *L. fuelleborni* is distinct along meristic canonical function two, with some overlap between *L. aurantinfra* and *L. candipygia*, new species (Fig. 7B).

Despite the overlap among *L. aurantinfra*, *L. candipygia*, new species, and *L. fuelleborni* along the canonical function axes, we found important distinctions among these species in the craniofacial region. Specifically, we examined the width to length ratios of both the lower jaw and snout.



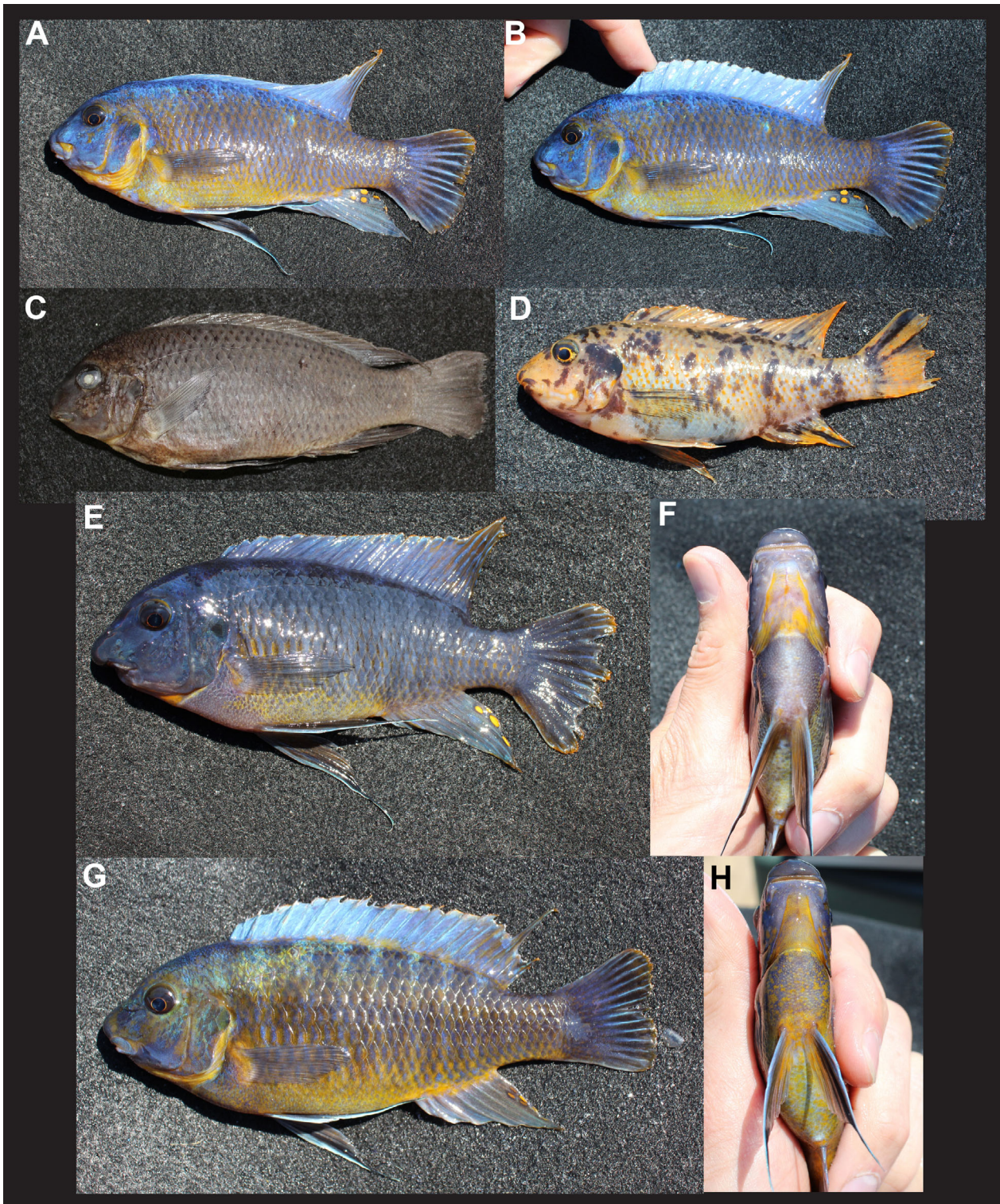


**Fig. 5.** *Labeotropheus aurantinfra*, new species. (A) Live male holotype (SAIAB 211375), 114.8 mm SL; (B) live holotype with dorsal fin elevated; (C) holotype after preservation; (D) live female paratype (MPM Fi50071) with 'orange-blotch' ('OB') color pattern, 88.7 mm SL; (E) live male paratype (MPM Fi50071) with gray blue coloration, 111.7 mm SL; (F) ventral surface of male from E showing orange throat and branchiostegals; (G) live male paratype (MPM Fi50071) with extensive orange pigmentation and green sheen on head and dorsum, 98.4 mm SL; (H) ventral surface of male from G showing orange throat and branchiostegals.

*Labeotropheus aurantinfra*, *L. candipygia*, new species, and *L. fuelleborni* all differ in these ratios (Fig. 8, Table 9).

**Distribution.**—*Labeotropheus aurantinfra* is endemic to Lake Malaŵi, along the Malaŵian shore. It appears to be restricted

to Chirwa Island and the nearby Ndomo Gap, between the tip of the Luromo Peninsula and Chirwa Island.

**Etymology.**—The specific epithet is a composite of the Latin adjective *aurantiacum*, meaning orange colored, and a second



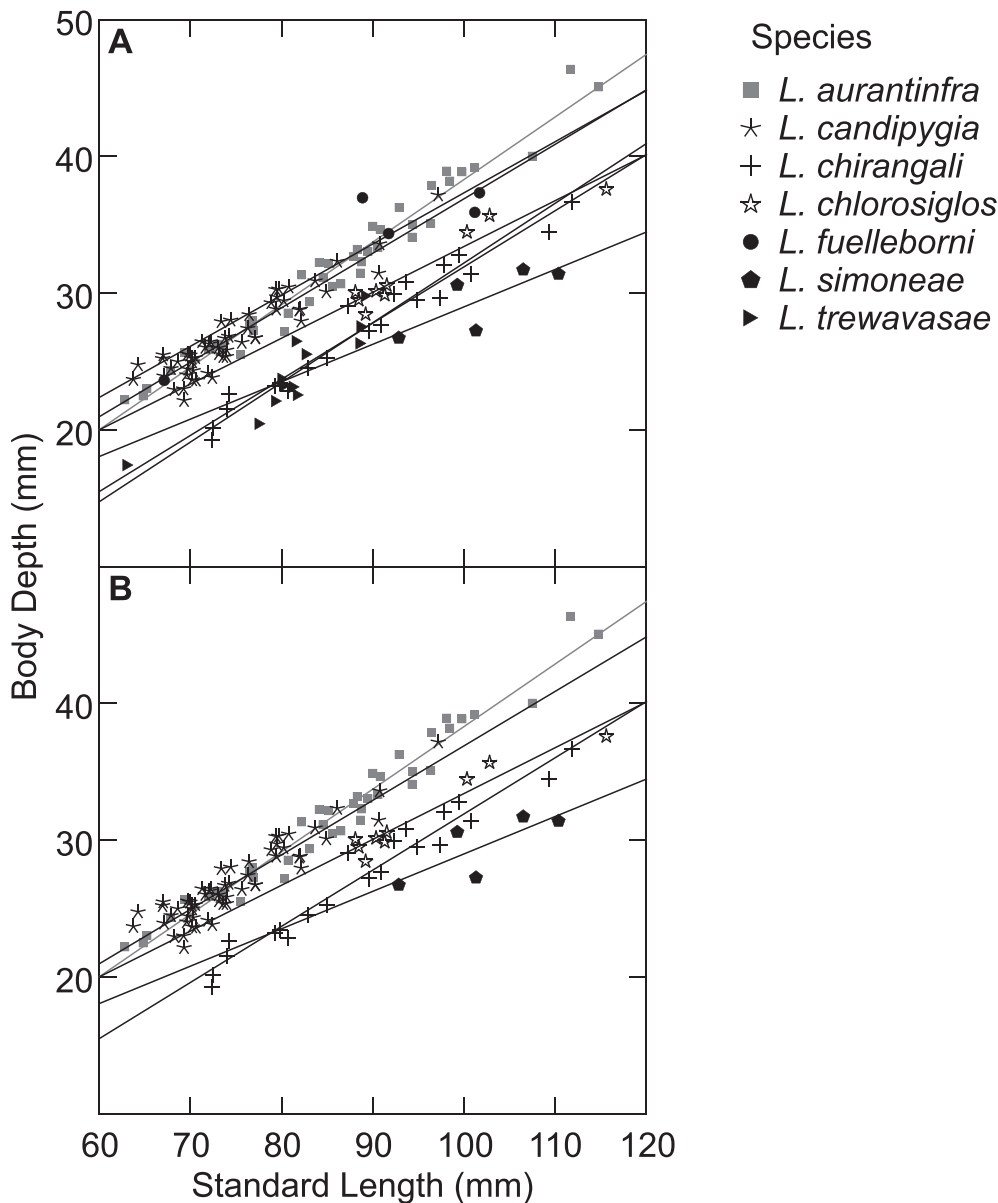


**Fig. 6.** Body depth–standard length relationships among *L. fuelleborni*, *L. trewavasae*, *L. chlorosiglos*, *L. simoneae*, and the three new species of *Labeotropheus* from the north-western portion of Lake Malaŵi. (A) All seven species; (B) same plot as A, but *L. fuelleborni* and *L. trewavasae* are omitted for clarity. The ANOVA accompanying these data is in Table 7.

Latin adjective, *infra*, meaning below or underneath. This is in reference to the unique male nuptial color pattern, in which the ventrum, anterior abdomen, and branchiostegals feature orange coloration.

***Labeotropheus candipygia*, Pauers and Phiri, new species**

urn:lsid:zoobank.org:act:2AF772CB-E420-4196-8FDE-B0EB728D68BE

Figures 6–9; Tables 7–10

**Holotype.**—SAIAB 211376, adult male, 82.1 mm SL, Malaŵi, Lake Malaŵi, Chitende Island, –10.3982807, 34.2579842, Michael J. Pauers, Titus B. Phiri, Victor Nantunga, and Shaibu Fisha, 31 July 2018.

**Paratypes.**—FMNH 145011, 1 male, 80.8 mm SL, 1 female, 86.1 mm SL, Malaŵi, Lake Malaŵi, Chitende Island, –10.3982807, 34.2579842, Michael J. Pauers, Titus B. Phiri, Victor Nantunga, and Shaibu Fisha, 31 July 2018; MPM Fi50067, 9 males, 8 females, 67.9–90.8 mm SL, Malaŵi, Lake

Malaŵi, Chitende Island, –10.3982807, 34.2579842, Michael J. Pauers, Titus B. Phiri, Victor Nantunga, and Shaibu Fisha, 31 July 2018; MPM Fi50068, 11 males, 8 females, 63.7–81.9 mm SL, Malaŵi, Lake Malaŵi, Chitende Island, –10.3982807, 34.2579842, Michael J. Pauers, Titus B. Phiri, Victor Nantunga, and Shaibu Fisha, 31 July 2018; MPM Fi50078, 7 males, 4 females, 64.2–97.2 mm SL, Malaŵi, Lake Malaŵi, Chitende Gap, –10.3975493, 34.2560859, Michael J. Pauers, Titus B. Phiri, Victor Nantunga, and Shaibu Fisha, 2 August 2018; SAIAB 211377, 1 male, 70.6 mm SL, 2 females, 70.2 and 74.4 mm SL, Malaŵi, Lake Malaŵi, Chitende Island, –10.3982807, 34.2579842, Michael J. Pauers, Titus B. Phiri, Victor Nantunga, and Shaibu Fisha, 31 July 2018.

**Diagnosis.**—*Labeotropheus candipygia* differs from all other species of *Labeotropheus* by the typical nuptial coloration of the males. Male *L. candipygia* have a distinct iridescent silvery-blue or silvery-white ventral surface; this unique coloration extends from the branchiostegals to the anus in all individuals, and will extend to through the caudal



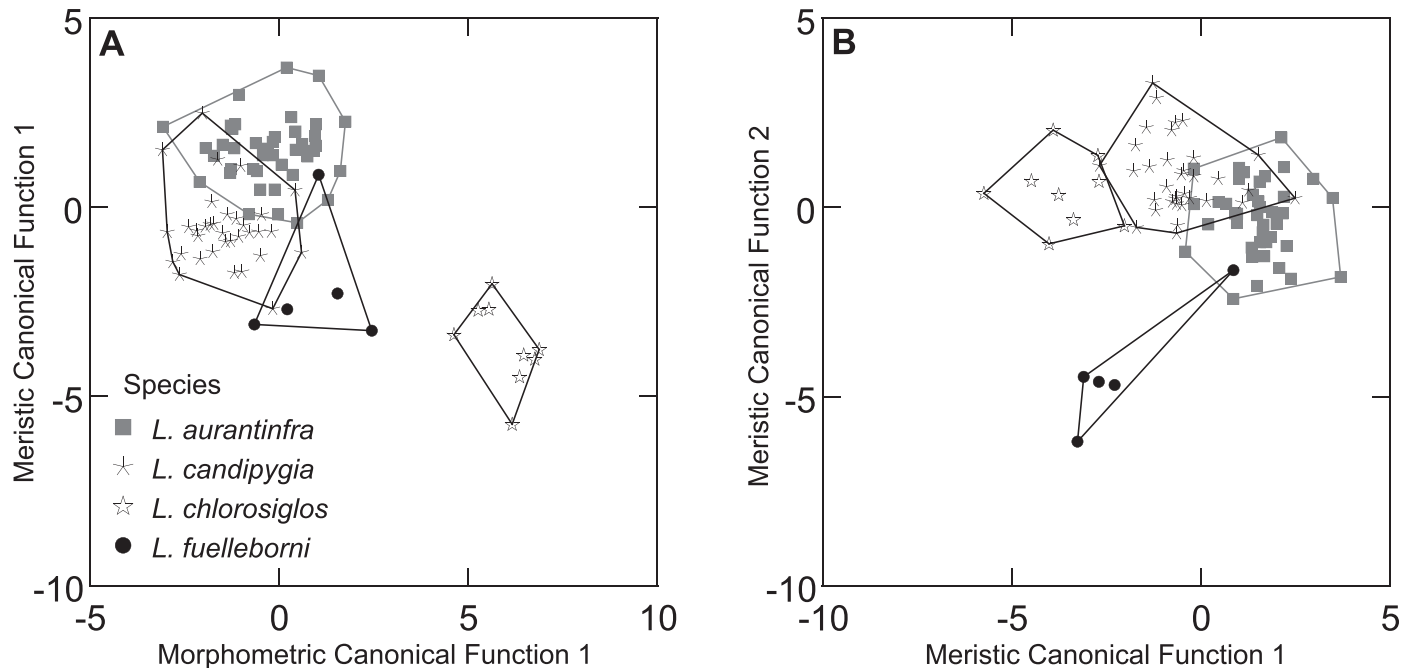


**Fig. 7.** Canonical function plots for the robust *Labeotropheus* from the Luromo Peninsula. (A) Morphometric canonical function 1 vs. meristic canonical function 1; (B) meristic canonical function 1 vs. meristic canonical function 2.

peduncle to the ventral attachment of the caudal fin in some individuals. Above this silvery-white ventrum, males are ochreous orange, which covers most of the head and can extend to the base of the dorsal fin, and extends posteriorly through the caudal peduncle to the base of the caudal fin, or they will be a dull grayish blue with ochreous-orange highlights on the scales of the dorsum. Both color patterns feature a brilliantly iridescent white dorsal fin that has ochreous-orange tips and patches of iridescent blue, black, orange, or red pigmentation.

*Labeotropheus candipygia* differs from the slender-bodied *Labeotropheus*, *L. trewasasae*, *L. simoneae*, *L. chirangali*, new species, except *L. rubidorsalis*, new species, due to its greater body depth (32.0–38.6% SL vs. 26.3–33.4% in *L. trewasasae*; 26.9–30.8% in *L. simoneae*; 26.6–33.2% in *L. chirangali*, new species); it does have a generally deeper body than *L. rubidorsalis*, new species, although the ranges overlap (31.6–36.1% in *L. rubidorsalis*, new species). It differs from *L. rubidorsalis*, new species, primarily in the nuptial coloration of the males, but also by a generally shorter snout length (19.7–33.9% HL vs. 29.8–42.7%), a longer snout pad (11.3–19.2% HL vs. mean 10.3–14.4%), and a greater number of tooth rows in the upper jaw (4–6 vs. 3–4).

In addition to the differences between *L. candipygia* and both *L. alticodia*, and *L. aurantinfra*, noted above, *L. candipygia* differs from the other robust-bodied *Labeotropheus* primarily via male nuptial coloration. While the morphometric and meristic values largely overlap with the other robust *Labeotropheus*, there are some distinctions. *Labeotropheus candipygia* has a greater distance between the tip of the snout and the origin of the dorsal fin (32.2–36.8% SL vs. 30.8–33.8%), a shorter distance between the insertion of the dorsal and anal fins (13.9–16.7% SL vs. 16.5–17.4%), and fewer teeth in the left side of the lower jaw (23–34 vs. 31–43) than *L. fuelleborni*. *Labeotropheus candipygia* typically has a shorter snout (19.7–33.9% HL vs. 25.2–40.8%), greater rostral

length (35.1–49.7% HL vs. 22.9–43.7%), and a larger snout pad (11.3–19.2% HL vs. 7.4–16.1%) than *L. artatorostris*. *Labeotropheus candipygia* has a narrower interorbital width (32.7–42.8% HL vs. 40.1–43.5%) and typically fewer infraorbital neuromasts (13–33 vs. 25–40) than *L. chlorosiglos*. Finally, *L. candipygia* differs from *L. obscurus*, new species, due to a shorter distance between the insertions of the dorsal and anal fins (13.9–16.7% SL vs. 15.8–17.8%), a shorter distance between the insertion of the dorsal fin and the origin of the anal fin (27.4–31.7% SL vs. 30.3–33.2%), a typically shorter lower jaw (21.5–39.4% HL vs. 27.6–40.4%), more rows of teeth in the upper jaw (4–6 vs. 3–4), more teeth in the left half of the lower jaw (23–34 vs. 20–26), and fewer infraorbital neuromasts (13–33 vs. 22–46).

**Description.**—Morphometric and meristic data summarized in Table 10. Body compressiform; ovoid shape. Body depth 32.0–38.6% SL; body consistently deep throughout its length. Body moderately wide at pectoral fin and opercular tab. Scales on belly and anterior abdomen cycloid and tightly crowded. Flank scales ctenoid; exposed portion of scale fan-shaped and approximately hexagonal. Anterior lateral line overlapping posterior lateral line by 0–3 scales. Dorsal fin long, with 16–19 spines and 7–10 rays. Origin of dorsal fin anterior to or opposite opercular tab. Dorsal rays 3, 4, 5 long, reaching beyond hypural to caudal fin. Anal fin angular and kite-shaped. Anal rays 3, 4, 5 long in most males and some females, reaching past caudal peduncle to caudal fin; most female specimens with short anal-fin rays, reaching only to caudal peduncle. Anal-fin origin opposite dorsal-fin spine 14, 15, or 16; anal-fin insertion anterior to or opposite dorsal-fin insertion. Caudal fin subtruncate. Pectoral fin rounded, 13–15 rays. Pelvic fin long, minimally reaching origin of anal fin and longer in the majority of specimens. Pelvic-fin ray slightly produced and filamentous in all males and most

**Table 6.** Morphometric and meristic values for *Labeotropheus aurantinfra*, new species ( $n = 42$ ).**(A) Morphometric data**

|  | Holotype | Mean $\pm$ SE   | Range      |
|--|----------|-----------------|------------|
| Standard length (SL, mm)                                     | 114.8    | 85.8 $\pm$ 1.9  | 62.8–114.8 |
| Head length (HL, mm)   | 33.5     | 26.6 $\pm$ 0.5  | 19.4–35.0  |
| % SL   |          |                 |            |
| HL   | 29.2     | 31.1 $\pm$ 0.2  | 29.1–37.8  |
| Snout to origin of dorsal fin (DFO)                          | 33.6     | 34.1 $\pm$ 0.2  | 31.8–37.4  |
| Snout to attachment of pelvic fins (PFO)                     | 37.3     | 39.7 $\pm$ 0.2  | 36.9–43.8  |
| Length of pectoral fin                                       | 24.9     | 24.1 $\pm$ 0.3  | 20.8–28.3  |
| Length of base of dorsal fin                                 | 63.0     | 59.7 $\pm$ 0.2  | 56.3–63.0  |
| DFO to origin of anal fin (AFO)                              | 56.3     | 52.9 $\pm$ 0.5  | 35.9–56.3  |
| Insertion of dorsal fin (DFI) to insertion of anal fin (AFI) | 17.8     | 15.5 $\pm$ 0.2  | 13.8–17.8  |
| DFO to AFI   | 69.6     | 63.8 $\pm$ 0.3  | 60.8–69.6  |
| DFI to AFO   | 32.4     | 29.7 $\pm$ 0.2  | 27.5–32.4  |
| DFI to ventral attachment of caudal fin                      | 18.9     | 18.2 $\pm$ 0.1  | 16.0–20.4  |
| AFI to dorsal attachment of caudal fin                       | 20.3     | 19.4 $\pm$ 0.2  | 17.3–22.2  |
| DFO to attachment of pelvic fins                             | 39.0     | 37.0 $\pm$ 0.2  | 33.4–40.4  |
| DFI to attachment of pelvic fins                             | 59.8     | 56.1 $\pm$ 0.3  | 51.4–59.8  |
| Body depth   | 39.3     | 36.9 $\pm$ 0.3  | 33.8–41.5  |
| Width at opercular tabs                                      | 18.0     | 17.3 $\pm$ 0.1  | 15.4–19.4  |
| Width at pectoral fins                                       | 16.1     | 15.7 $\pm$ 0.2  | 13.2–18.9  |
| Width at pelvic fins   | 8.3      | 7.3 $\pm$ 0.1   | 5.8–8.6    |
| % HL   |          |                 |            |
| Eye diameter   | 25.4     | 27.3 $\pm$ 0.3  | 23.5–32.4  |
| Preorbital depth   | 30.0     | 26.5 $\pm$ 0.3  | 21.3–31.7  |
| Cheek depth  | 29.8     | 26.1 $\pm$ 0.4  | 22.1–32.0  |
| Snout length   | 32.6     | 30.4 $\pm$ 0.3  | 26.7–33.1  |
| Rostral length   | 47.3     | 45.3 $\pm$ 0.5  | 36.1–51.1  |
| Upper jaw length (UJL)                                       | 21.0     | 20.1 $\pm$ 0.3  | 15.2–23.5  |
| Snout pad length   | 13.3     | 15.1 $\pm$ 0.3  | 10.5–19.4  |
| Lower jaw length (LJL)                                       | 25.3     | 27.3 $\pm$ 0.4  | 22.5–31.6  |
| Lower jaw width (LJW)  | 51.1     | 44.5 $\pm$ 0.4  | 37.1–51.1  |
| Head depth   | 112.1    | 104.1 $\pm$ 0.9 | 86.0–116.6 |
| Interorbital width   | 46.8     | 42.0 $\pm$ 0.5  | 30.5–47.8  |
| Snout width  | 41.8     | 38.2 $\pm$ 0.4  | 31.5–44.6  |

**(B) Meristic data**

|                                      | Holotype | Mode | Range |
|--------------------------------------|----------|------|-------|
| Anterior lateral line scales (LLS)   | 24       | 23   | 19–25 |
| Posterior LLS                        | 11       | 12   | 9–14  |
| Overlapping LLS                      | 1        | 1    | 0–3   |
| Dorso-lateral scale rows             | 8        | 8    | 7–10  |
| Pectoro-pelvic scale rows            | 10       | 11   | 9–12  |
| Cheek scale rows                     | 3        | 3    | 3–4   |
| Dorsal-fin spines (DFS)              | 19       | 18   | 17–19 |
| Dorsal-fin rays (DFR)                | 8        | 9    | 7–10  |
| Anal-fin spines (AFS)                | 3        | 3    | –     |
| Anal-fin rays (AFR)                  | 7        | 8    | 7–9   |
| Pectoral-fin rays                    | 14       | 14   | 12–14 |
| Pelvic-fin rays                      | 6        | 6    | –     |
| Upper jaw teeth rows                 | 5        | 5    | 4–6   |
| Lower jaw teeth rows                 | 6        | 5    | 1–7   |
| Teeth on left lower jaw              | 35       | 30   | 24–37 |
| Teeth on left dentigerous premaxilla | 8        | 7    | 5–11  |
| Total gill rakers                    | 12       | 12   | 10–15 |
| Epibranchial gill rakers             | 3        | 2    | 1–3   |
| Ceratobranchial gill rakers          | 8        | 9    | 7–10  |
| Infraorbital pores                   | 9        | 9    | 8–10  |
| Neuromasts within infraorbital pores | 48       | 23   | 15–67 |

**Table 7.** Analysis of variance on body depth vs. standard length for northwestern *Labeotropheus*.

| (A) Analysis of variance ( $n = 150$ ; multiple $R^2 = 0.948$ ) |                |     |             |         |              |  |
|---|----------------|-----|-------------|---------|--------------|--|
| Variable  | Sum of squares | df  | Mean square | $F$     | $P$          |  |
| Species   | 18.587         | 6   | 3.098       | 2.139   | 0.053        |  |
| Standard length   | 652.909        | 1   | 652.909     | 450.789 | $\leq 0.001$ |  |
| Species * standard length                                       | 20.715         | 6   | 3.452       | 2.384   | 0.032        |  |
| Error   | 196.979        | 135 | 1.448       |         |              |  |

| (B) Pairwise comparisons: * $P \leq 0.05$ ; ** $P \leq 0.01$ ; *** $P \leq 0.001$ ; <sup>ns</sup> = not significant |                       |                      |                      |                        |                       |                     |
|---|-----------------------|----------------------|----------------------|------------------------|-----------------------|---------------------|
|   | <i>L. aurantinfra</i> | <i>L. candipygia</i> | <i>L. chirangali</i> | <i>L. chlorosiglos</i> | <i>L. fuelleborni</i> | <i>L. simoneae</i>  |
| <i>L. candipygia</i>  | -0.405 <sup>ns</sup>  |                      |                      |                        |                       |                     |
| <i>L. chirangali</i>  | -5.594***             | -5.188***            |                      |                        |                       |                     |
| <i>L. chlorosiglos</i>  | -2.819**              | -2.414*              | 2.774**              |                        |                       |                     |
| <i>L. fuelleborni</i>   | 0.443 <sup>ns</sup>   | 0.849 <sup>ns</sup>  | 6.037***             | 3.263*                 |                       |                     |
| <i>L. simoneae</i>  | -6.186*               | -5.781*              | -0.592 <sup>ns</sup> | -3.367 <sup>ns</sup>   | -6.630*               |                     |
| <i>L. trewavasae</i>  | -5.742***             | -5.337***            | -0.149 <sup>ns</sup> | -2.923**               | -6.186***             | 0.444 <sup>ns</sup> |

females; produced and non-filamentous in some females. Pelvic-fin attachment opposite dorsal-fin spine 4, 5, or 6.

Head long (29.8–35.3% SL) and relatively shallow. Strongly curved profile with slight concavity above eye and prominent snout. Snout short but wide with long snout pad (11.3–19.2% HL). Cheek compact with 2–6 scale rows. Infraorbital pores 9 or 10 with 13–35 neuromasts among them. Oral jaws short and wide. Oral teeth tricuspid and closely set on both upper and lower jaws; 4–11 tricuspid teeth on lateral portion of left upper jaw. Gill rakers stout, triangular, and widely spaced; 6–10 ceratobranchial and 1–3 epibranchial gill rakers on first gill arch. All specimens with 1 raker between the cerato- and epibranchial rakers.

**Coloration of males.**—Ground color pale blue, fading to silvery blue or silvery white across ventral surface of head and flank; snout, jaws, operculum, throat, anterior abdomen, ventrum, and ventral portion of caudal peduncle all silvery blue or silvery white. All portions of head, operculum, flank, and caudal peduncle dorsal to the dorsal attachment of pectoral fin with ochreous-orange coloration; scales of flank and caudal peduncle either entirely ochreous orange or ringed with ochreous orange around pale blue or silvery blue center of scale. Opercular tab black, sometimes with faint greenish sheen. Ground color of dorsal-fin membrane silvery blue or silvery white, sometimes overlain by red patches throughout fin, or by ochreous-orange patches along proximal portion. Tips of dorsal fin ochreous orange. Caudal fin blue or silvery blue, grading to black posteriorly; thin orange trailing edge. Anal fin white or bluish white, with 3–5 orange-yellow eggspots. Pelvic fin pale red posteriorly with bright white leading edge; thick black band between white leading edge and posterior red color.

In preservative, males uniformly dark brown or gray with 11 faint vertical bars visible across flank and caudal peduncle on some specimens.

**Coloration of females.**—Head, body, and caudal peduncle uniformly light brown, with 11 faint dark bars extending across flank and caudal peduncle. Opercular tab black. Scales of flank and caudal peduncle with small orange spots close to insertion of scale. Throat and branchiostegals orange. Dorsal fin brownish gray with orange tips and orange trailing edge. Caudal fin brownish gray with thin orange trailing edge.

Anal fin brownish gray with 1–2 yellow eggspots and orange trailing edge. Pelvic fin pale orange posteriorly with bright white leading edge; thick black band between white leading edge and posterior orange color.

In preservative, females uniformly dark brown or gray with 11 faint vertical bars visible across flank and caudal peduncle on some specimens.

**Multivariate analyses.**—Due to the overlap of morphometric and meristic characteristics between *L. candipygia* and the other *Labeotropheus*, we compared the body depth–standard length ratios of *L. candipygia* and its geographically proximate congeners (Fig. 6). This ratio clearly places *L. candipygia* within the robust *Labeotropheus*, and distinguishes it from the slender *L. simoneae* and *L. chirangali*, new species, as well as the intermediate *L. chlorosiglos* (Table 7). We also performed canonical discriminant function analyses on the meristic and  $\log_{10}$ -transformed morphological data for *L. candipygia*, *L. chlorosiglos*, *L. fuelleborni*, and the geographically proximate *L. aurantinfra*. The canonical discriminant function analyses were robust and significant (Table 8). While *L. chlorosiglos* is distinct along the first morphometric canonical function, and *L. fuelleborni* is particularly distinct along the second meristic canonical function, *L. candipygia* and *L. aurantinfra* overlap along all three canonical functions we plotted (Fig. 7). Despite the lack of resolution between *L. candipygia* and *L. aurantinfra* based upon the canonical discriminant function analyses, we found that *L. candipygia* has smaller width to length ratios of both the lower jaw and snout than both *L. aurantinfra* and *L. fuelleborni* (Fig. 8, Table 9).

**Distribution.**—*Labeotropheus candipygia* is endemic to the Malaŵian shore of Lake Malaŵi, and appears to be restricted to Chitende Island and the nearby Chitende Gap, between Chitende Point (the remnants of a peninsula that once connected Chitende Island to the mainland) and Chitende Island.

**Remarks.**—Ribbink et al. (1983a) state that they found the males of the robust *Labeotropheus* at Chitende Island to have a sky blue head, dorsum, and body, with an orange chest and dorsal fin. We did not find any robust *Labeotropheus* at Chitende matching this description; indeed, this description seems most similar to *L. aurantinfra* from Chirwa Island.

**Table 8.** Canonical discriminant function (CDF) analyses on (A)  $\text{Log}_{10}$ -transformed morphometric and (B) meristic data for *L. aurantinfra*, *L. candipygia*, *L. chlorosiglos*, and *L. fueleborni*. Standardized functions are reported. Uninformative variables are omitted.

(A)  $\text{Log}_{10}$ -transformed morphometric data: Wilks'  $\lambda = 0.038$ ,  $F_{39,219} = 11.382$ ,  $P \leq 0.001$

|  | CDF 1  | CDF 2  | CDF 3  |
|--|--------|--------|--------|
| Eigenvalue                                       | 4.619  | 1.528  | 0.855  |
| Canonical correlation                            | 0.907  | 0.777  | 0.679  |
| HL   | 0.988  | 1.074  | 1.698  |
| Snout to attachment of pelvic fins               | 1.775  | -0.831 | -0.744 |
| Insertion of dorsal fin to insertion of anal fin | 1.705  | 1.153  | -1.429 |
| Origin of dorsal fin to insertion of anal fin    | 0.309  | 0.294  | 2.982  |
| Body depth                                       | -2.970 | -0.479 | -1.250 |
| Width at opercular tabs                          | -1.565 | -1.905 | -0.512 |
| Preorbital depth                                 | -0.402 | -1.106 | -1.344 |
| Cheek depth                                      | -0.383 | 1.349  | 0.507  |
| Snout length                                     | 0.838  | -1.293 | -0.247 |
| Rostral length                                   | -1.549 | -0.026 | 0.261  |
| Lower jaw length (LJL)                           | -0.777 | 0.240  | -0.607 |
| Lower jaw width (LJW)                            | 0.095  | 1.753  | -0.779 |
| Interorbital width                               | 2.057  | -0.431 | 1.081  |
| Species means                                    |        |        |        |
| <i>L. aurantinfra</i>                            | -0.221 | -1.281 | -0.081 |
| <i>L. candipygia</i>                             | -1.442 | 1.173  | 0.437  |
| <i>L. chlorosiglos</i>                           | 5.966  | 0.722  | 0.689  |
| <i>L. fueleborni</i>                             | 0.922  | 1.486  | -3.535 |

(B) Meristic data: Wilks'  $\lambda = 0.052$ ,  $F_{60,200} = 5.654$ ,  $P \leq 0.001$

|                                      | CDF 1  | CDF 2  | CDF 3  |
|--------------------------------------|--------|--------|--------|
| Eigenvalue                           | 2.872  | 1.418  | 1.069  |
| Canonical correlation                | 0.859  | 0.766  | 0.719  |
| Anterior lateral line scales (LLS)   | 0.305  | 0.228  | 0.433  |
| Posterior LLS                        | -0.343 | 0.138  | -0.207 |
| Overlapping LLS                      | -0.083 | 0.023  | -0.327 |
| Dorso-lateral scale rows             | -0.749 | 0.454  | -0.443 |
| Pectoro-pelvic scale rows            | 1.082  | -0.326 | -0.352 |
| Cheek scale rows                     | -0.199 | 0.299  | -0.319 |
| Dorsal-fin spines (DFS)              | 0.181  | 0.141  | 0.288  |
| Dorsal-fin rays (DFR)                | -0.072 | 0.124  | 0.099  |
| Anal-fin rays (AFR)                  | 0.037  | 0.476  | -0.304 |
| Pectoral-fin rays                    | -0.131 | -0.122 | 0.091  |
| Pelvic-fin rays                      | 0.029  | -0.185 | 0.091  |
| Upper jaw teeth rows                 | -0.181 | 0.058  | 0.402  |
| Lower jaw teeth rows                 | -0.176 | -0.153 | -0.399 |
| Teeth on left lower jaw              | -0.290 | -0.921 | 0.099  |
| Teeth on left dentigerous premaxilla | -0.453 | 0.037  | 0.140  |
| Total gill rakers                    | -0.112 | 0.526  | 0.111  |
| Epibranchial gill rakers             | 0.052  | -0.144 | -0.028 |
| Ceratobranchial gill rakers          | 0.408  | -0.185 | 0.279  |
| Infraorbital pores                   | -0.003 | 0.206  | 0.148  |
| Neuromasts within infraorbital pores | -0.020 | 0.200  | 0.120  |
| Species means                        |        |        |        |
| <i>L. aurantinfra</i>                | 1.478  | -0.255 | 0.541  |
| <i>L. candipygia</i>                 | -0.556 | 0.841  | -1.016 |
| <i>L. chlorosiglos</i>               | -3.634 | 0.417  | 2.017  |
| <i>L. fueleborni</i>                 | -2.097 | -4.326 | -1.261 |

Interestingly, they describe the slender *Labeotropheus* at Chitende as having coloration similar to that of *L. candipygia* (Ribbink et al., 1983a, 1983b). We did not find any slender *Labeotropheus* at Chitende; *L. candipygia* was the only species of *Labeotropheus* present.

**Etymology.**—The specific epithet combines the Latin adjective for white or brilliant, *candidum*, and the New Latin noun *pygia*, meaning rump or buttocks. This refers to the bright white or bluish-white ventrum of the males.

***Labeotropheus chirangali*, Pauers and Phiri, new species**  
urn:lsid:zoobank.org:act:F4B4749E-26C3-4C2F-BB47-09AC6CFEF06D

Figures 6, 10, 11; Tables 7, 11, 12

**Holotype.**—SAIAB 211378, adult male, 97.8 mm SL, Malaŵi, Lake Malaŵi, Mphanga Rocks, -10.4328123, 34.2783040, Michael J. Pauers, Titus B. Phiri, Victor Nantunga, and Stuart M. Grant, Ltd, crew, 1 August 2018.

**Paratypes.**—FMNH 145012, 1 male, 94.9 mm SL, 1 female, 100.8 mm SL, Malaŵi, Lake Malaŵi, Mphanga Rocks, -10.4328123, 34.2783040, Michael J. Pauers, Titus B. Phiri, Victor Nantunga, and Stuart M. Grant, Ltd, crew, 1 August 2018; MPM Fi50076, 12 males, 3 females, 72.4–109.4 mm SL, Malaŵi, Lake Malaŵi, Mphanga Rocks, -10.4328123, 34.2783040, Michael J. Pauers, Titus B. Phiri, Victor Nantunga, and Stuart M. Grant, Ltd, crew, 1 August 2018; SAIAB 211379, 1 male, 92.3 mm SL, 2 females, 74.3 and 84.9 mm SL, Malaŵi, Lake Malaŵi, Mphanga Rocks, -10.4328123, 34.2783040, Michael J. Pauers, Titus B. Phiri, Victor Nantunga, and Stuart M. Grant, Ltd, crew, 1 August 2018.

**Diagnosis.**—*Labeotropheus chirangali* differs from the robust *Labeotropheus*, except *L. chlorosiglos* and *L. candipygia*, due to its slender body (26.6–33.2% SL vs. 35.2–41.6% in *L. fueleborni*; 33.8–41.5% in *L. aurantinfra*; 35.2–41.5% in *L. obscurus*, new species; 37.4–40.6% in *L. alticodia*; and 34.3–42.0% in *L. artatorostris*). *Labeotropheus chirangali* has a slenderer body than *L. chlorosiglos* and *L. candipygia*, although its range of body depth partially overlaps with those of these species (31.9–34.7% in *L. chlorosiglos*; 31.9–38.6% in *L. candipygia*). There are additional morphometric differences between *L. chirangali* and both *L. chlorosiglos* and *L. candipygia*, although some of the ranges overlap. *Labeotropheus chirangali* differs from both *L. chlorosiglos* and *L. candipygia* by shorter distances between the tip of the snout and the origin of the dorsal fin (28.4–32.7% SL vs. 31.2–34.4% in *L. chlorosiglos*; 32.2–36.8% in *L. candipygia*), between the origin of the dorsal fin and the origin of the anal fin (32.2–51.5% SL vs. 51.3–54.6% in *L. chlorosiglos*; 47.6–54.0% in *L. candipygia*), and between the origin of the dorsal fin and the attachment of the pelvic fins (28.6–33.4% SL vs. 33.0–36.0% in *L. chlorosiglos*; 32.7–38.8% in *L. candipygia*). Additionally, *L. chirangali* has a greater width between the opercular tabs (15.1–17.8% HL vs. 14.7–15.7%) than *L. chlorosiglos*.

*Labeotropheus chirangali* differs from the other slender-bodied *Labeotropheus* primarily due to the nuptial coloration of the males. Male *L. chirangali* have a dark blue head, flank, and ventrum, and the scales in this region may have small ochreous-orange highlights. Above this extensive dark blue



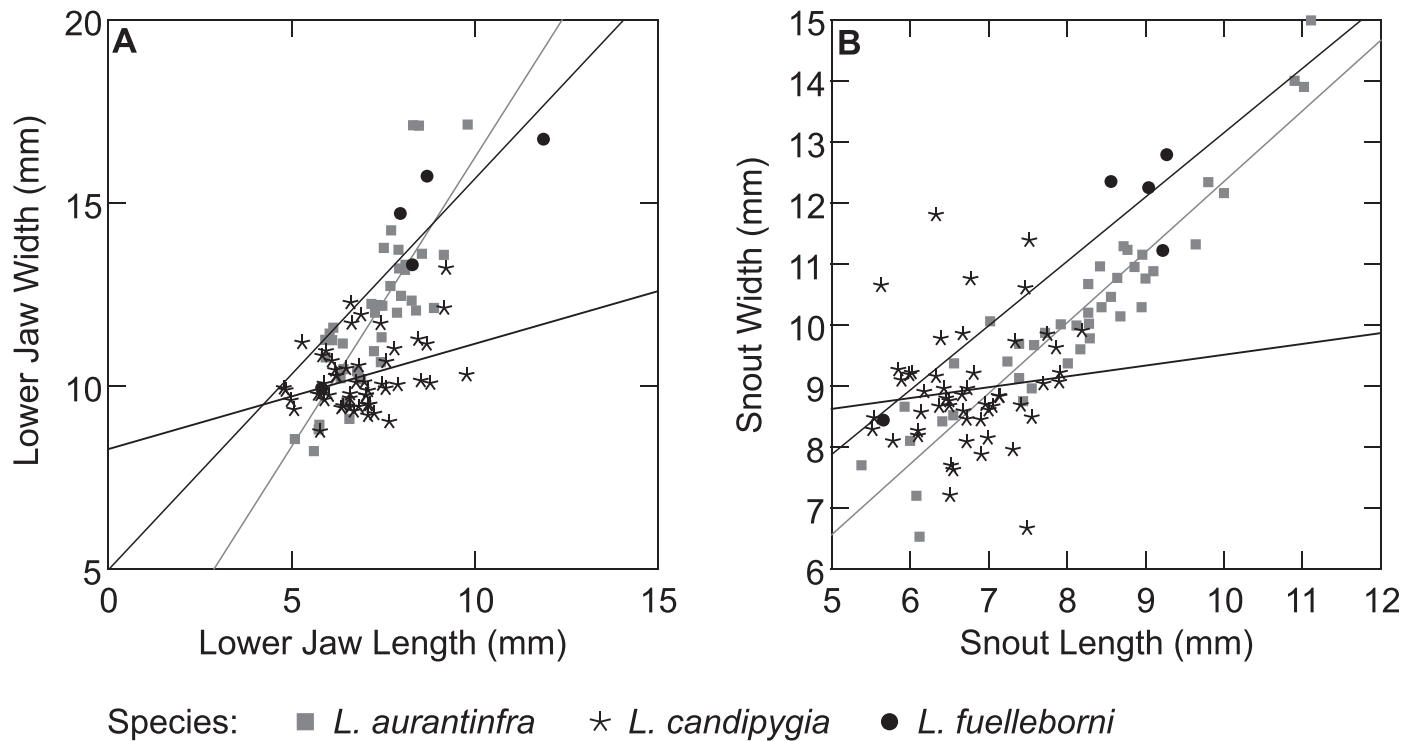


**Fig. 8.** Comparison of jaw and snout dimensions among *L. fuelleborni* and the two newly described robust *Labeotropheus* from northwestern Lake Malaŵi. (A) Lower jaw length versus lower jaw width; (B) snout length versus snout width. The ANOVA accompanying these data is in Table 9.

patch, male *L. chirangali* have a bright sky-blue dorsum; this pigmentation extends onto the dorsal fin. The tips of the dorsal fin are yellow, as is the trailing edge of this fin; the anal fin and the pelvic fins are the same bright sky blue as the dorsal fin. Many of the morphometric and meristic values of *L. chirangali* overlap with those of the other slender *Labeotropheus*, although there are some distinctions. *Labeotropheus chirangali* differs from *L. trewavasae* due to a larger snout pad (13.6–19.4% HL vs. 10.3–14.2%), a wider lower jaw

(39.0–49.5% HL vs. 34.7–43.9%), fewer rows of teeth in the lower jaw (3–5 vs. 5–6), and more infraorbital neuromasts (14–38 vs. 8–25). *Labeotropheus chirangali* differs from *L. simoneae* due to a greater rostral length (39.2–47.6% HL vs. 34.3–43.0%), a larger snout pad (13.6–19.4% HL vs. mean 9.5–15.9%), and fewer overlapping lateral line scales (0–3 vs. 4–5). Finally, *L. chirangali* differs from *L. rubidorsalis*, new species, due to a smaller distance between the tip of the snout and the origin of the dorsal fin (28.4–32.7% SL vs. 31.4–

**Table 9.** Analysis of variance of lower jaw and snout width in *Labeotropheus aurantinfra*, *L. candipygia*, and *L. fuelleborni*.

| (A) Lower jaw width ( $n = 99$ ; multiple $R^2 = 0.698$ )          |                       |    |             |                      |              |  |
|--|-----------------------|----|-------------|----------------------|--------------|--|
| Variable   | Sum of squares        | df | Mean square | F                    | P            |  |
| Lower jaw length   | 96.107                | 1  | 96.107      | 81.864               | $\leq 0.001$ |  |
| Species  | 32.472                | 2  | 16.236      | 13.830               | $\leq 0.001$ |  |
| Lower jaw length * species   | 46.256                | 2  | 23.128      | 19.700               | $\leq 0.001$ |  |
| Error  | 109.180               | 93 | 1.174       |                      |              |  |
| Pairwise comparisons: * $P \leq 0.001$ ; $^{ns}$ = not significant |                       |    |             |                      |              |  |
|  | <i>L. aurantinfra</i> |    |             | <i>L. candipygia</i> |              |  |
| <i>L. candipygia</i>   | 1.338*                |    |             |                      |              |  |
| <i>L. fuelleborni</i>  | 0.903 $^{ns}$         |    |             | 2.241*               |              |  |
| (B) Snout width ( $n = 99$ ; multiple $R^2 = 0.730$ )              |                       |    |             |                      |              |  |
| Variable   | Sum of squares        | df | Mean square | F                    | P            |  |
| Snout length   | 34.684                | 1  | 34.684      | 52.274               | $\leq 0.001$ |  |
| Species  | 16.487                | 2  | 8.243       | 12.424               | $\leq 0.001$ |  |
| Snout length * species   | 16.744                | 2  | 8.372       | 12.618               | $\leq 0.001$ |  |
| Error  | 61.706                | 93 | 0.664       |                      |              |  |
| Pairwise comparisons: * $P \leq 0.01$ ; $^{ns}$ = not significant  |                       |    |             |                      |              |  |
|  | <i>L. aurantinfra</i> |    |             | <i>L. candipygia</i> |              |  |
| <i>L. candipygia</i>   | -0.303 $^{ns}$        |    |             |                      |              |  |
| <i>L. fuelleborni</i>  | 1.067 $^{ns}$         |    |             | 1.369*               |              |  |



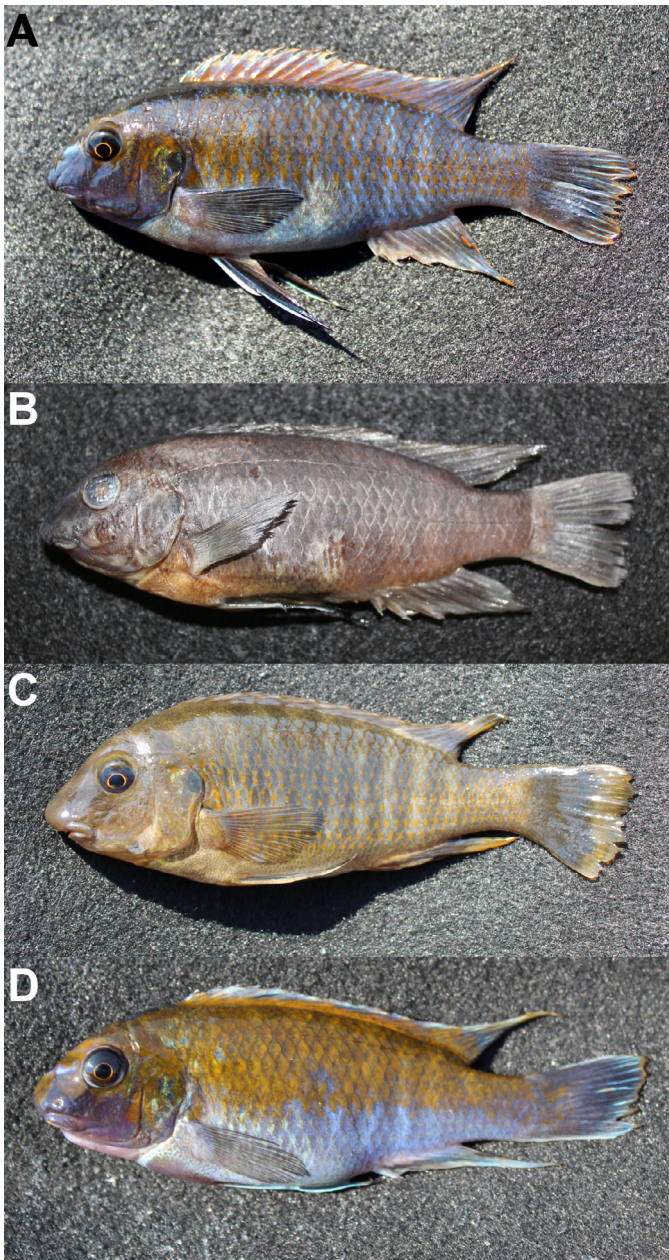


**Fig. 9.** *Labeotropheus candipygia*, new species. (A) Live male holotype (SAIAB 211376) from Chitende Island, 82.1 mm SL; (B) holotype after preservation; (C) live female paratype (MPM Fi50067) from Chitende Island, 90.8 mm SL; (D) live male paratype (MPM Fi50078) from Chitende Gap, 67.1 mm SL.

35.0%), a greater distance between the insertion of the dorsal fin and the attachment of the pelvic fins (54.1–58.8% SL vs. 49.5–55.1%), a smaller preorbital depth (23.4–28.4% HL vs. 26.6–32.9%), a larger snout pad (13.6–19.4% HL vs. 10.3–14.2%), and a greater number of ceratobranchial gill rakers (7–10 vs. 5–8).

**Description.**—Morphometric data and meristic summarized in Table 11. Body compressiform and slender; body depth 27.5–30.3% SL. Flattened ovoid body shape, slightly deeper anteriorly than posteriorly. Body wide, slightly cylindrical in transverse cross section. Scales on belly and anterior abdomen cycloid and tightly crowded. Flank scales ctenoid;

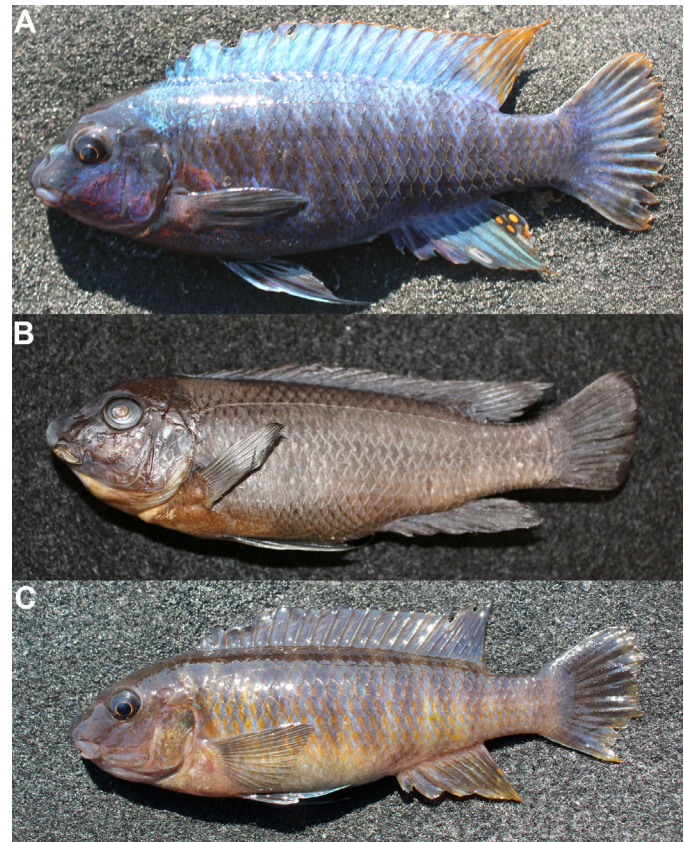


**Fig. 10.** *Labeotropheus chirangali*, new species. (A) Live male holotype (SAIAB 211378), 97.8 mm SL; (B) holotype after preservation; (C) live female paratype (MPM Fi50076), 84.9 mm SL.

exposed portion of scale fan-shaped and approximately hexagonal. Anterior lateral line overlapping posterior lateral line by 0–3 scales. Dorsal fin of typical length for a *Labeotropheus* (55.8–61.3% SL), 18–19 spines and 8–9 rays. Origin of dorsal fin posterior to or overlapping opercular tab. Dorsal-fin rays 3, 4, 5 long, reaching to hypural and beyond to caudal fin. Anal fin angular anteriorly with slight rounding to membrane posteriorly. Origin of anal fin opposite dorsal-fin spine 16; insertion of anal fin variable (anterior, opposite, or posterior) with respect to insertion of dorsal fin. Anal-fin rays 3, 4, 5 reach past hypural in most males; these only reach to mid-caudal peduncle in females. Caudal fin subtruncate. Pectoral fin short (19.3–24.7% SL), rounded, 13–14 rays. Pelvic fin long, minimally reaching origin of anal fin and longer in the majority of specimens. Pelvic-fin ray slightly produced and filamentous in males and females. Pelvic-fin attachment opposite dorsal-fin spine 4 or 5.

Head short but deep for a slender *Labeotropheus*. Head profile moderately to strongly concave with prominent snout. Snout of typical length but wide (34.7–40.2% HL) with protruding snout pad (13.6–19.4% HL). Cheek with 3 scale rows. Infraorbital pores 9–10, with 14–38 neuromasts among them. Oral jaws long and wide. Oral teeth tricuspid and closely set on both upper and lower jaws; 6–11 tricuspid teeth on lateral portion of left upper jaw. Gill rakers stout, triangular, and widely spaced; 7–10 ceratobranchial and 1–3 epibranchial gill rakers on first gill arch. All specimens with 1 raker between the cerato- and epibranchial rakers.



**Table 10.** Morphometric and meristic values for *Labeotropheus candipygia*, new species ( $n = 57$ ).

| <b>(A) Morphometric data</b>                                 |          |                |            |
|--|----------|----------------|------------|
|  | Holotype | Mean $\pm$ SE  | Range      |
| Standard length (SL, mm)                                     | 82.1     | 76.4 $\pm$ 1.3 | 64.3–97.2  |
| Head length (HL, mm)   | 26.0     | 24.5 $\pm$ 0.4 | 21.2–31.0  |
| % SL   |          |                |            |
| HL   | 31.7     | 32.0 $\pm$ 0.1 | 29.8–35.3  |
| Snout to origin of dorsal fin (DFO)                          | 33.0     | 34.3 $\pm$ 0.1 | 32.3–36.8  |
| Snout to attachment of pelvic fins (PFO)                     | 38.5     | 39.6 $\pm$ 0.2 | 35.6–42.4  |
| Length of pectoral fin                                       | 23.2     | 24.0 $\pm$ 0.2 | 20.3–27.8  |
| Length of base of dorsal fin                                 | 61.7     | 58.9 $\pm$ 0.2 | 55.5–61.8  |
| DFO to origin of anal fin (AFO)                              | 50.6     | 51.6 $\pm$ 0.2 | 47.6–54.0  |
| Insertion of dorsal fin (DFI) to insertion of anal fin (AFI) | 15.6     | 15.3 $\pm$ 0.1 | 13.9–16.7  |
| DFO to AFI   | 64.0     | 62.8 $\pm$ 0.3 | 50.6–66.8  |
| DFI to AFO   | 30.7     | 29.7 $\pm$ 0.1 | 27.4–31.7  |
| DFI to ventral attachment of caudal fin                      | 18.1     | 18.5 $\pm$ 0.1 | 16.0–20.1  |
| AFI to dorsal attachment of caudal fin                       | 18.5     | 19.4 $\pm$ 0.1 | 17.8–21.8  |
| DFO to attachment of pelvic fins                             | 34.9     | 35.6 $\pm$ 0.2 | 32.7–38.8  |
| DFI to attachment of pelvic fins                             | 55.7     | 54.8 $\pm$ 0.2 | 50.9–58.8  |
| Body depth   | 35.2     | 35.9 $\pm$ 0.2 | 32.0–38.6  |
| Width at opercular tabs                                      | 16.7     | 16.5 $\pm$ 0.1 | 14.7–18.4  |
| Width at pectoral fins                                       | 16.2     | 15.0 $\pm$ 0.1 | 12.6–17.1  |
| Width at pelvic fins   | 7.3      | 7.5 $\pm$ 0.1  | 6.3–8.6    |
| % HL   |          |                |            |
| Eye diameter   | 22.3     | 26.9 $\pm$ 0.2 | 22.3–30.7  |
| Preorbital depth   | 25.5     | 24.8 $\pm$ 0.2 | 18.2–30.3  |
| Cheek depth  | 27.8     | 25.6 $\pm$ 0.3 | 21.1–30.6  |
| Snout length   | 22.5     | 28.5 $\pm$ 0.4 | 19.7–33.9  |
| Rostral length   | 43.0     | 43.4 $\pm$ 0.4 | 35.1–49.7  |
| Upper jaw length (UJL)                                       | 19.6     | 19.7 $\pm$ 0.2 | 14.9–22.6  |
| Snout pad length   | 15.3     | 15.9 $\pm$ 0.2 | 11.3–19.2  |
| Lower jaw length (LJL)                                       | 23.9     | 28.7 $\pm$ 0.5 | 21.5–39.4  |
| Lower jaw width (LJW)  | 39.5     | 43.4 $\pm$ 0.3 | 37.7–48.6  |
| Head depth   | 97.0     | 99.2 $\pm$ 0.6 | 87.9–108.1 |
| Interorbital width   | 35.4     | 37.6 $\pm$ 0.3 | 32.7–42.8  |
| Snout width  | 35.6     | 37.8 $\pm$ 0.3 | 30.2–42.6  |
| <b>(B) Meristic data</b>                                     |          |                |            |
|  | Holotype | Mode           | Range      |
| Anterior lateral line scales (LLS)                           | 24       | 23             | 20–25      |
| Posterior LLS  | 13       | 12             | 10–15      |
| Overlapping LLS  | 2        | 2              | 0–3        |
| Dorso-lateral scale rows                                     | 8        | 9              | 8–11       |
| Pectoro-pelvic scale rows                                    | 11       | 10             | 8–12       |
| Cheek scale rows   | 3        | 4              | 2–6        |
| Dorsal-fin spines (DFS)                                      | 17       | 17             | 16–19      |
| Dorsal-fin rays (DFR)  | 9        | 9              | 7–10       |
| Anal-fin spines (AFS)  | 3        | 3              | –          |
| Anal-fin rays (AFR)  | 8        | 8              | 7–9        |
| Pectoral-fin rays  | 14       | 14             | 13–15      |
| Pelvic-fin rays  | 6        | 6              | –          |
| Upper jaw teeth rows   | 5        | 5              | 4–6        |
| Lower jaw teeth rows   | 6        | 5              | 3–7        |
| Teeth on left lower jaw                                      | 27       | 27             | 23–34      |
| Teeth on left dentigerous premaxilla                         | 7        | 8              | 4–11       |
| Total gill rakers  | 12       | 12             | 10–14      |
| Epibranchial gill rakers                                     | 3        | 2              | 1–3        |
| Ceratobranchial gill rakers                                  | 8        | 8              | 6–10       |
| Infraorbital pores   | 9        | 9              | 9–10       |
| Neuromasts within infraorbital pores                         | 15       | 22             | 13–35      |

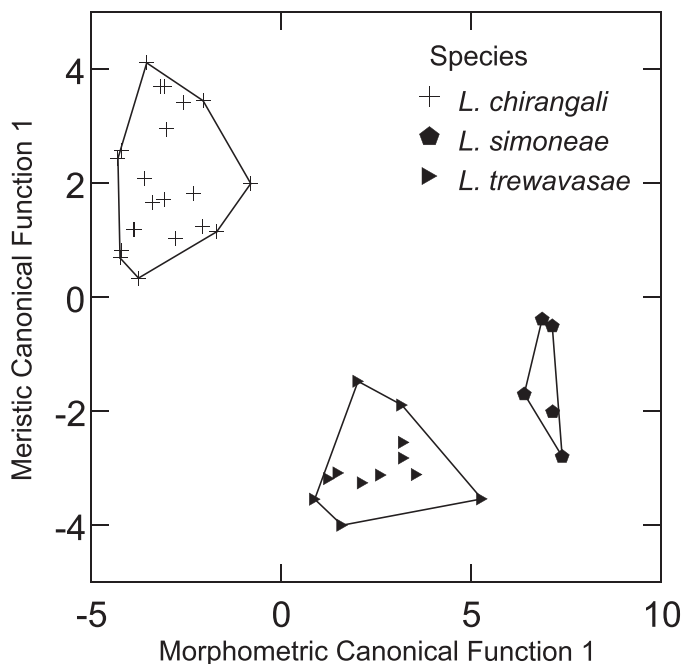


**Fig. 11.** Plot of morphometric canonical function 1 vs. meristic canonical function 1 for *L. chirangali*, *L. simoneae*, and *L. trewavasae*.

**Coloration of males.**—Head and dorsum blue, varying among individuals from dark navy blue to lighter sky blue. Ground color of scales along flank and caudal peduncle blue, typically matching head and dorsum; i.e., males with sky blue head and dorsum have sky blue ground color along flank. Opercular tab black with metallic green sheen. 11 dark blue-black bars along flank and caudal peduncle. Scales along flank and caudal peduncle typically with ochreous-orange dots near inserted portion, generally becoming more prominent on caudal peduncle; some individuals with ochreous orange on caudal peduncle only. Dorsal fin blue, matching blue color of dorsum; trailing edge and tips of dorsal fin ochreous orange. Caudal fin blue suffused with orange; trailing edge ochreous orange. Anal fin iridescent bluish white or bluish gray with 3–6 orange-yellow eggspots. Posterior portion of pelvic fin very pale orange with white leading edge; prominent black stripe between leading edge and posterior pigment.

In preservative, males uniformly gray or brown with 11 dark bars spanning flank and caudal peduncle.

**Coloration of females.**—Head and operculum brown; opercular tab black with faint green sheen. Ground color of flank and caudal peduncle light tan; 11 dark brown bars span flank and caudal peduncle. Scales of flank and peduncle with small orange dot near insertion of scale. Belly white. Dorsal fin grayish brown or gray. Caudal fin gray; thin orange trailing edge. Spinous portion of anal fin white or gray, rayed portion grayish brown with orange trailing edge; 1–2 small orange-yellow eggspots present on rayed portion of anal fin. Pelvic fin pale orange with white leading edge; thin black bar separates leading edge from posterior pigment.

In preservative, females uniformly dark brown or gray with 11 faint vertical bars visible across flank and peduncle on some specimens.

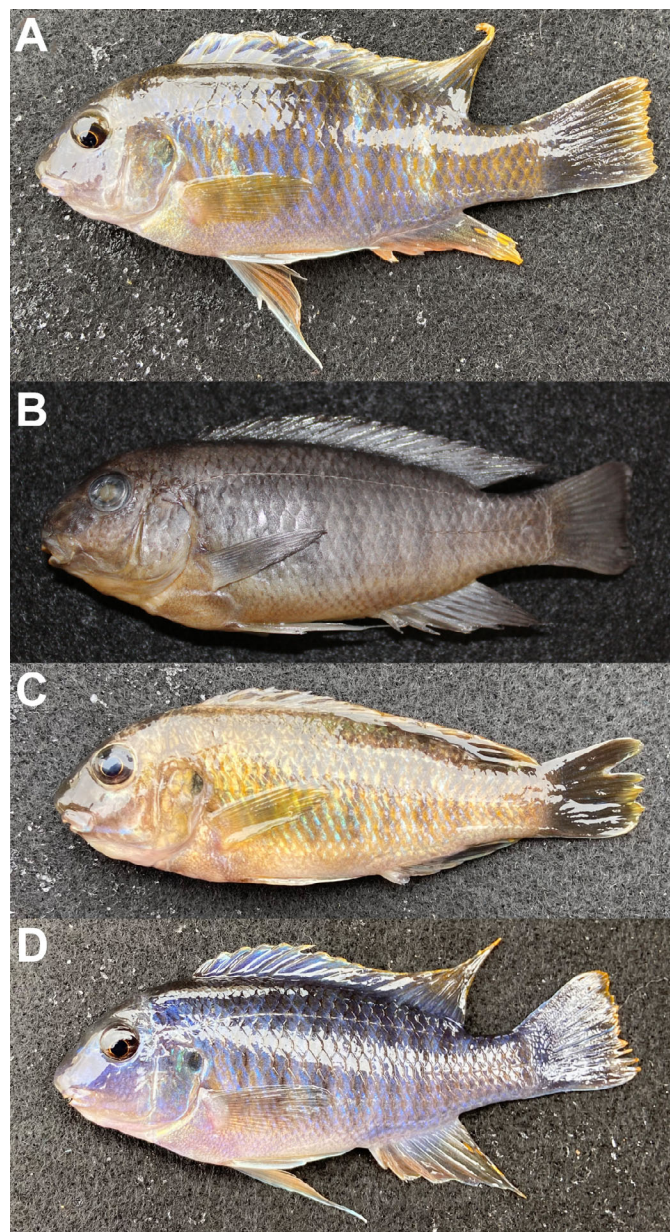


**Fig. 12.** *Labeotropheus obscurus*, new species. (A) Live male holotype (SAIAB 211380), 78.2 mm SL; (B) holotype after preservation; (C) live female paratype (FMNH 145013), 75.6 mm SL; (D) live male paratype (FMNH 145013), 78.3 mm SL, displaying a primarily blue color pattern.

**Multivariate analyses.**—Due to the overlap of morphometric and meristic characteristics between *L. chirangali* and the other geographically proximate slender *Labeotropheus*, we performed canonical discriminant function analyses on the meristic and  $\text{Log}_{10}$ -transformed morphometric data of *L. chirangali*, *L. simoneae*, and *L. trewavasae*. These analyses were robust and significant (Table 12). When the first morphological canonical function is plotted against the first meristic canonical function, *L. chirangali* is clearly distinct from *L. simoneae* and *L. trewavasae* (Fig. 11).

**Distribution.**—*Labeotropheus chirangali* is endemic to the Malaŵian shore of Lake Malaŵi, and is known only from the Mphanga Rocks off the tip of the Luromo Peninsula along the northwestern shore of the lake.



**Table 11.** Morphometric and meristic values for *Labeotropheus chirangali*, new species ( $n = 21$ ).

| <b>(A) Morphometric data</b>                                 |          |          |            |
|--|----------|----------|------------|
|  | Holotype | Mean±SE  | Range      |
| Standard length (SL, mm)                                     | 97.8     | 88.8±2.5 | 72.4–111.8 |
| Head length (HL, mm)   | 26.9     | 25.6±0.7 | 20.3–32.3  |
| % SL   |          |          |            |
| HL   | 27.5     | 28.8±0.2 | 28.8–30.3  |
| Snout to origin of dorsal fin (DFO)                          | 30.0     | 30.4±0.2 | 30.4–32.7  |
| Snout to attachment of pelvic fins (PFO)                     | 38.8     | 38.3±0.2 | 38.3–40.1  |
| Length of pectoral fin                                       | 20.7     | 22.1±0.3 | 22.1–24.7  |
| Length of base of dorsal fin                                 | 58.7     | 58.9±0.3 | 58.9–61.3  |
| DFO to origin of anal fin (AFO)                              | 49.7     | 46.9±1.3 | 46.9–51.5  |
| Insertion of dorsal fin (DFI) to insertion of anal fin (AFI) | 15.2     | 14.5±0.1 | 14.5–15.7  |
| DFO to AFI   | 62.2     | 60.7±0.7 | 60.7–63.7  |
| DFI to AFO   | 29.2     | 28.0±0.2 | 28.0–29.8  |
| DFI to ventral attachment of caudal fin                      | 18.5     | 17.7±0.2 | 17.7–19.1  |
| AFI to dorsal attachment of caudal fin                       | 19.4     | 18.7±0.2 | 18.7–20.0  |
| DFO to attachment of pelvic fins                             | 32.9     | 31.1±0.3 | 31.1–33.4  |
| DFI to attachment of pelvic fins                             | 55.9     | 56.1±0.2 | 56.1–58.8  |
| Body depth   | 32.8     | 30.6±0.4 | 30.6–33.3  |
| Width at opercular tabs                                      | 16.8     | 16.2±0.2 | 16.2–17.8  |
| Width at pectoral fins                                       | 16.3     | 14.9±0.2 | 14.9–16.6  |
| Width at pelvic fins   | 7.2      | 7.0±0.1  | 7.0–7.6    |
| % HL   |          |          |            |
| Eye diameter   | 27.3     | 26.3±0.3 | 26.3–28.4  |
| Preorbital depth   | 27.5     | 25.7±0.3 | 25.7–28.4  |
| Cheek depth  | 25.2     | 25.9±0.6 | 25.9–33.2  |
| Snout length   | 31.8     | 29.9±0.6 | 29.9–34.3  |
| Rostral length   | 45.9     | 44.8±0.5 | 44.8–47.6  |
| Upper jaw length (UJL)                                       | 20.8     | 20.9±0.3 | 20.9–23.7  |
| Snout pad length   | 15.0     | 15.7±0.4 | 15.7–19.4  |
| Lower jaw length (LJL)                                       | 41.5     | 32.1±1.1 | 32.1–41.5  |
| Lower jaw width (LJW)  | 44.7     | 42.4±0.6 | 42.4–49.5  |
| Head depth   | 105.6    | 97.1±0.9 | 97.1–105.6 |
| Interorbital width   | 44.0     | 39.4±0.6 | 39.4–44.0  |
| Snout width  | 39.6     | 37.1±0.3 | 37.1–40.2  |
| <b>(B) Meristic data</b>                                     |          |          |            |
|  | Holotype | Mode     | Range      |
| Anterior lateral line scales (LLS)                           | 24       | 24       | 23–25      |
| Posterior LLS  | 12       | 13       | 11–15      |
| Overlapping LLS  | 1        | 2        | 0–3        |
| Dorso-lateral scale rows                                     | 9        | 9        | 7–11       |
| Pectoro-pelvic scale rows                                    | 11       | 12       | 9–13       |
| Cheek scale rows   | 4        | 3        | 2–4        |
| Dorsal-fin spines (DFS)                                      | 18       | 18       | 18–19      |
| Dorsal-fin rays (DFR)  | 8        | 8        | 8–9        |
| Anal-fin spines (AFS)  | 3        | 3        | –          |
| Anal-fin rays (AFR)  | 8        | 8        | 7–9        |
| Pectoral-fin rays  | 13       | 14       | 13–14      |
| Pelvic-fin rays  | 6        | 6        | –          |
| Upper jaw teeth rows   | 5        | 4        | 3–6        |
| Lower jaw teeth rows   | 4        | 4        | 3–5        |
| Teeth on left lower jaw                                      | 31       | 23       | 22–35      |
| Teeth on left dentigerous premaxilla                         | 9        | 8        | 6–11       |
| Total gill rakers  | 12       | 12       | 9–13       |
| Epibranchial gill rakers                                     | 3        | 2        | 1–3        |
| Ceratobranchial gill rakers                                  | 8        | 9        | 7–10       |
| Infraorbital pores   | 9        | 9        | 9–10       |
| Neuromasts within infraorbital pores                         | 34       | 32       | 14–38      |

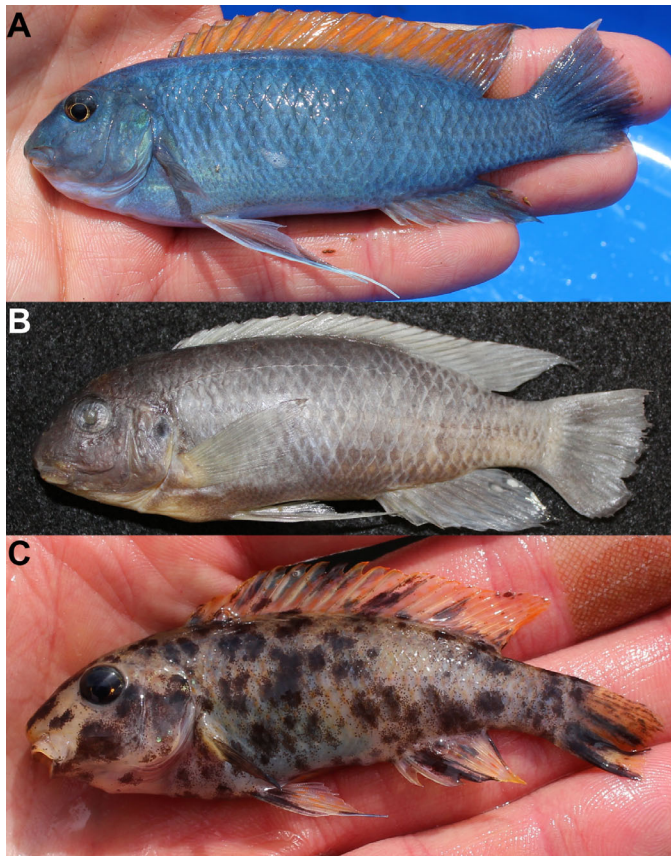


**Fig. 13.** *Labeotropheus rubidorsalis*, new species. (A) Live male holotype (SAIAB 211383), 91.2 mm SL; (B) holotype after preservation; (C) live female paratype (MPM Fi50090), 69.4 mm SL.

**Etymology.**—*Chirangali* is the Chichewa word for beacon, referring to the navigational beacon present on Mphanga Rocks.

***Labeotropheus obscurus*, Phiri and Pauers, new species**

urn:lsid:zoobank.org:act:EC803C63-127B-43AE-AD0F-8A73A1DDD6DB

Figures 3, 4, 12; Tables 4, 5, 13

**Holotype.**—SAIAB 211380, adult male, 78.2 mm SL, Malaŵi, Lake Malaŵi, Namalenje Island, -13.730081, 34.641074, Michael J. Pauers, Titus B. Phiri, and Sanudi Likupe, 15 January 2020.

**Paratypes.**—FMNH 145013, 1 male, 78.3 mm SL, 1 female, 75.6 mm SL, Malaŵi, Lake Malaŵi, Namalenje Island, -13.730081, 34.641074, Michael J. Pauers, Titus B. Phiri, and Sanudi Likupe, 15 January 2020; MPM Fi50080, 1 male, 68.1 mm SL, 3 females, 63.6, 66.6, and 67.2 mm SL, Malaŵi, Lake Malaŵi, Namalenje Island, -13.730081, 34.641074, Michael J. Pauers, Titus B. Phiri, and Sanudi Likupe, 15 January 2020; MPM Fi50091, 2 males, 5 females, 64.0–70.2 mm SL, Malaŵi, Lake Malaŵi, Namalenje Island, -13.730788, 34.640388, Michael J. Pauers, Titus B. Phiri, and Sanudi Likupe, 17 January 2020; MPM Fi50091, 1 male, 4 females, 65.9–71.8 mm SL, Malaŵi, Lake Malaŵi, Namalenje Island, -13.729377, 34.640478, Michael J. Pauers, Titus B. Phiri, and Sanudi Likupe, 17 January 2020; SAIAB 211381, 1 male, 66.1

**Table 12.** Canonical discriminant function (CDF) analyses on (A)  $\text{Log}_{10}$ -transformed morphometric and (B) meristic data for *L. chirangali*, *L. simoneae*, and *L. trewavasae*. Standardized functions are reported. Uninformative variables are omitted.

(A)  $\text{Log}_{10}$ -transformed morphometric data: Wilks'  $\lambda = 0.012$ ,  $F_{22,50} = 18.350$ ,  $P \leq 0.001$

|  | CDF 1  | CDF 2  |
|--|--------|--------|
| Eigenvalue   | 15.034 | 4.135  |
| Canonical correlation                                | 0.968  | 0.897  |
| SL   | 6.083  | 4.038  |
| HL   | 2.563  | -3.347 |
| Snout to attachment of pelvic fins                   | -2.512 | 1.166  |
| Insertion of dorsal fin to insertion of anal fin     | 2.196  | 2.746  |
| Origin of dorsal fin to attachment of pelvic fins    | -2.860 | -3.362 |
| Insertion of dorsal fin to attachment of pelvic fins | -6.286 | -4.607 |
| Preorbital depth                                     | 2.135  | -0.039 |
| Rostral length                                       | -2.692 | 0.597  |
| Upper jaw length                                     | -1.205 | -0.232 |
| Lower jaw width (LJW)                                | 2.940  | 1.112  |
| Interorbital width                                   | -0.849 | 2.363  |
| Species means  |        |        |
| <i>L. chirangali</i>                                 | -3.118 | 0.639  |
| <i>L. simoneae</i>                                   | 6.990  | 3.420  |
| <i>L. trewavasae</i>                                 | 2.544  | -2.544 |

(B) Meristic data: Wilks'  $\lambda = 0.047$ ,  $F_{36,36} = 3.597$ ,  $P \leq 0.001$

|                                      | CDF 1  | CDF 2  |
|--------------------------------------|--------|--------|
| Eigenvalue                           | 5.866  | 2.078  |
| Canonical correlation                | 0.924  | 0.822  |
| Anterior lateral line scales (LLS)   | 0.533  | 0.633  |
| Posterior LLS                        | 0.575  | -0.10  |
| Overlapping LLS                      | -0.679 | 0.477  |
| Dorso-lateral scale rows             | 0.466  | -0.356 |
| Pectoro-pelvic scale rows            | 0.030  | -0.737 |
| Cheek scale rows                     | 0.196  | -0.162 |
| Dorsal-fin spines (DFS)              | -0.639 | -0.753 |
| Dorsal-fin rays (DFR)                | -0.637 | -1.251 |
| Anal-fin rays (AFR)                  | 0.489  | -0.730 |
| Pectoral-fin rays                    | 0.138  | 0.978  |
| Upper jaw teeth rows                 | -0.365 | -0.220 |
| Lower jaw teeth rows                 | -0.380 | 0.021  |
| Teeth on left lower jaw              | -0.440 | 0.449  |
| Teeth on left dentigerous premaxilla | 0.303  | -0.053 |
| Total gill rakers                    | 0.237  | 0.471  |
| Epibranchial gill rakers             | -0.338 | -0.501 |
| Infraorbital pores                   | 0.675  | 0.330  |
| Neuromasts within infraorbital pores | 0.666  | 0.663  |
| Species means                        |        |        |
| <i>L. chirangali</i>                 | 2.051  | -0.243 |
| <i>L. simoneae</i>                   | -1.484 | 3.443  |
| <i>L. trewavasae</i>                 | -2.971 | -1.010 |

mm SL, 1 female, 51.4 mm SL, Malaŵi, Lake Malaŵi, Namalenje Island, -13.730081, 34.641074, Michael J. Pauers, Titus B. Phiri, and Sanudi Likupe, 17 January 2020.

**Diagnosis.**—*Labeotropheus obscurus* differs from all other species of *Labeotropheus* due to the unusually drab and muted coloration of sexually mature males; male nuptial

**Table 13.** Morphometric and meristic values for *Labeotropheus obscurus*, new species ( $n = 21$ ).

| <b>(A) Morphometric data</b>                                 |          |                 |             |
|--|----------|-----------------|-------------|
|  | Holotype | Mean $\pm$ SE   | Range       |
| Standard length (SL, mm)                                     | 78.2     | 68.4 $\pm$ 1.0  | 60.8–78.3   |
| Head length (HL, mm)   | 22.9     | 21.4 $\pm$ 0.3  | 19.1–25.2   |
| % SL   |          |                 |             |
| HL   | 29.2     | 31.3 $\pm$ 0.2  | 29.2–37.8   |
| Snout to origin of dorsal fin (DFO)                          | 31.4     | 33.4 $\pm$ 0.2  | 31.4–37.4   |
| Snout to attachment of pelvic fins (PFO)                     | 42.4     | 42.2 $\pm$ 0.4  | 38.8–45.9   |
| Length of pectoral fin                                       | 23.6     | 25.0 $\pm$ 0.2  | 22.8–28.3   |
| Length of base of dorsal fin                                 | 59.2     | 58.3 $\pm$ 0.2  | 56.1–63.0   |
| DFO to origin of anal fin (AFO)                              | 51.6     | 52.3 $\pm$ 0.2  | 50.8–56.3   |
| Insertion of dorsal fin (DFI) to insertion of anal fin (AFI) | 17.0     | 16.8 $\pm$ 0.1  | 15.8–17.8   |
| DFO to AFI   | 63.6     | 62.9 $\pm$ 0.2  | 61.6–69.6   |
| DFI to AFO   | 31.4     | 31.3 $\pm$ 0.1  | 30.3–33.2   |
| DFI to ventral attachment of caudal fin                      | 19.1     | 19.4 $\pm$ 0.2  | 17.7–21.4   |
| AFI to dorsal attachment of caudal fin                       | 21.6     | 19.9 $\pm$ 0.2  | 18.3–22.2   |
| DFO to attachment of pelvic fins                             | 38.0     | 37.7 $\pm$ 0.3  | 35.4–40.4   |
| DFI to attachment of pelvic fins                             | 57.3     | 55.0 $\pm$ 0.2  | 53.7–59.8   |
| Body depth   | 37.7     | 37.8 $\pm$ 0.3  | 35.2–41.5   |
| Width at opercular tabs                                      | 17.3     | 16.9 $\pm$ 0.1  | 15.8–19.4   |
| Width at pectoral fins                                       | 16.0     | 15.5 $\pm$ 0.2  | 13.8–18.9   |
| Width at pelvic fins   | 8.6      | 8.1 $\pm$ 0.1   | 7.1–8.7     |
| % HL   |          |                 |             |
| Eye diameter   | 27.3     | 29.8 $\pm$ 0.3  | 27.3–32.4   |
| Preorbital depth   | 27.5     | 25.8 $\pm$ 0.6  | 20.1–31.7   |
| Cheek depth  | 32.1     | 28.4 $\pm$ 0.5  | 25.0–32.8   |
| Snout length   | 29.7     | 29.5 $\pm$ 0.3  | 27.2–33.1   |
| Rostral length   | 41.7     | 41.3 $\pm$ 0.4  | 38.0–51.1   |
| Upper jaw length (UJL)                                       | 22.7     | 20.6 $\pm$ 0.3  | 17.5–23.5   |
| Snout pad length   | 14.1     | 12.2 $\pm$ 0.4  | 9.5–19.4    |
| Lower jaw length (LJL)                                       | 39.2     | 35.0 $\pm$ 0.7  | 27.7–40.4   |
| Lower jaw width (LJW)  | 44.6     | 42.6 $\pm$ 0.4  | 38.4–51.1   |
| Head depth   | 115.3    | 105.7 $\pm$ 0.9 | 100.0–116.6 |
| Interorbital width   | 38.5     | 35.8 $\pm$ 0.4  | 32.3–47.8   |
| Snout width  | 38.9     | 35.8 $\pm$ 0.5  | 30.9–44.6   |
| <b>(B) Meristic data</b>                                     |          |                 |             |
|  | Holotype | Mode            | Range       |
| Anterior lateral line scales (LLS)                           | 23       | 23              | 21–25       |
| Posterior LLS  | 15       | 12              | 11–15       |
| Overlapping LLS  | 4        | 2               | 0–4         |
| Dorso-lateral scale rows                                     | 9        | 9               | 8–10        |
| Pectoro-pelvic scale rows                                    | 11       | 11              | 10–13       |
| Cheek scale rows   | 4        | 3               | 3–4         |
| Dorsal-fin spines (DFS)                                      | 16       | 17              | 16–18       |
| Dorsal-fin rays (DFR)  | 9        | 8               | 7–9         |
| Anal-fin spines (AFS)  | 3        | 3               | –           |
| Anal-fin rays (AFR)  | 7        | 8               | 7–8         |
| Pectoral-fin rays  | 14       | 14              | 13–15       |
| Pelvic-fin rays  | 6        | 6               | –           |
| Upper jaw teeth rows   | 4        | 3               | 3–4         |
| Lower jaw teeth rows   | 4        | 4               | 3–5         |
| Teeth on left lower jaw                                      | 22       | 22              | 20–26       |
| Teeth on left dentigerous premaxilla                         | 9        | 9               | 4–10        |
| Total gill rakers  | 9        | 12              | 9–14        |
| Epibranchial gill rakers                                     | 2        | 2               | 1–3         |
| Ceratobranchial gill rakers                                  | 6        | 8               | 6–11        |
| Infraorbital pores   | 9        | 9               | 9–9         |
| Neuromasts within infraorbital pores                         | 32       | 29              | 22–46       |



color pattern dominated by gray and brown pigmentation, with some blue and orange highlights on scales and fins, as opposed to a nuptial color pattern dominated by blue, orange, or red pigmentation.

*Labeotropheus obscurus* differs from the slender-bodied *Labeotropheus*, *L. trewavasae*, *L. simoneae*, and *L. chirangali*, but not *L. rubidorsalis*, new species, due to its greater body depth (35.2–41.5% SL vs. 26.3–33.4% in *L. trewavasae*; 26.9–30.8% in *L. simoneae*; and 26.6–33.2% in *L. chirangali*). *Labeotropheus obscurus* typically has a greater body depth than *L. rubidorsalis*, new species, although the ranges slightly overlap (31.6–36.1% SL in *L. rubidorsalis*, new species). Overall, *L. obscurus* does have a deeper body than *L. rubidorsalis*, new species, as indicated by several other measurements akin to body depth, including the distance between the origin of the dorsal fin and the origin of the anal fin (50.8–56.3% SL vs. 45.6–50.3%), the distance between the insertion of the dorsal fin and the insertion of the anal fin (15.8–17.8% SL vs. 13.5–15.7%), the distance between the insertion of the dorsal fin and the origin of the anal fin (30.3–33.2% vs. 27.6–30.3%), and the distance between the origin of the dorsal fin and the attachment of the pelvic fins (35.4–40.5% SL vs. 31.5–35.4%).

*Labeotropheus obscurus* has a distinctly larger eye diameter than several of the robust species of *Labeotropheus* (27.3–32.4% HL vs. 23.7–26.6% in *L. fuelleborni*; 22.6–25.5% in *L. chlorosiglos*; and 24.9–27.5% in *L. alticodia*). It also has fewer rows of teeth in the upper jaw than all robust *Labeotropheus* except *L. alticodia* (3–4 vs. 4–5 in *L. fuelleborni*; 5–7 in *L. chlorosiglos*; 5–8 in *L. artatorostris*; 4–6 in *L. aurantinfra*; and 4–6 in *L. candipygia*), and fewer teeth in the left side of the lower jaw (20–26) than *L. fuelleborni* (31–43), *L. chlorosiglos* (30–37), and *L. alticodia* (29–35).

**Description.**—Morphometric and meristic data summarized in Table 13. Body compressiform; body shape ovoid. Body depth 35.2–41.5% SL and consistently deep throughout trunk. Body relatively narrow at pectoral fin and opercular tab. Scales on belly and anterior abdomen cycloid and tightly crowded. Flank scales ctenoid; exposed portion of scale fan-shaped and approximately hexagonal. Anterior lateral line overlapping posterior lateral by 0–4 scales. Dorsal fin 56.1–63.0% SL, 16–18 spines and 7–9 rays. Origin of dorsal fin overlapping opercular tab. Dorsal-fin rays 3, 4, 5 long, reaching to hypural and beyond to caudal fin. Anal-fin shape variable; angular and kite-like in some (6 of 19) specimens, angled anteriorly with slight rounding to membrane posteriorly in others (13 of 19). Origin of anal fin opposite dorsal-fin spine 16 in majority of specimens; insertion of anal fin variable (anterior, opposite, or posterior) with respect to insertion of dorsal fin. Anal-fin rays 3, 4, 5 reach past hypural in most males; these only reach to mid-caudal peduncle in females. Caudal fin subtruncate. Pectoral fin long (22.8–28.3% SL), rounded, with 13–15 rays. Pelvic fin long, minimally reaching origin of anal fin and longer in the majority of specimens. Pelvic-fin ray slightly produced and filamentous in all males and most females; pelvic-fin ray is non-filamentous in some females. Pelvic-fin attachment opposite dorsal-fin spine 5 or 6 in most specimens; opposite dorsal-fin spine 4 in one specimen.

Head long (29.2–37.8% SL), depth typical for *Labeotropheus*. Head profile moderately to strongly curved with slightly protruding snout. Snout long but narrow; snout

width 30.9–44.6% HL with slight snout pad (9.5–19.4% HL). Cheek with 3–4 scale rows. Infraorbital pores 9, with 22–46 neuromasts among them. Oral jaws long and narrow. Oral teeth tricuspid and closely set on both upper and lower jaws; 4–10 tricuspid teeth on lateral portion of left upper jaw. Gill rakers stout, triangular, and widely spaced; 6–11 ceratobranchial and 1–3 epibranchial gill rakers on first gill arch. All specimens with 1 raker between the cerato- and epibranchial rakers.

**Coloration of males.**—Ground color of head, operculum, flank, and caudal peduncle gray. Flank suffused with pale blue in some individuals; 11 darker bars extending across flank and peduncle visible in some individuals. Scales of flank abdominal to lateral line, between operculum and caudal peduncle, with orange spots near insertion of scale. Opercular tab black, overlain with metallic blue in some individuals. Dorsal fin gray in most individuals, pale blue in males with pale blue flanks; dorsal fin with orange tips and thin orange trailing edge in all individuals. Caudal fin gray with orange trailing edge. Anal fin predominantly gray with orange pigment on spinous portion; rayed portion with yellow tips and trailing edge, 2–4 orange-yellow eggspots present. Pelvic fin orange with white leading edge.

Preserved males uniformly brown or dark gray with 11 dark bars spanning flank and caudal peduncle visible on some individuals.

**Coloration of females.**—Head, body, and caudal peduncle uniformly light gray, with 11 faint dark bars extending across flank and caudal peduncle; some individuals suffused with a faint metallic green. Scales of flank and caudal peduncle with small orange spots close to insertion of scale. Opercular tab black. Throat and branchiostegals white. Dorsal fin white with orange tips; some specimens with orange trailing edge. Caudal fin brownish gray, some specimens with orange trailing edge. Rayed portion of anal fin pale brownish gray with 1–2 yellow eggspots; spinous portion white. Pelvic fin pale orange, with bright white leading edge.

In preservative, females uniformly dark brown or gray with 11 faint vertical bars visible across flank and caudal peduncle on some specimens.

**Multivariate analyses.**—Due to the overlap of morphometric and meristic characteristics between *L. obscurus* and the other *Labeotropheus*, we compared the body depth–standard length ratios of *L. obscurus* and its geographically proximate congeners (Fig. 3). This ratio clearly places *L. obscurus* with the robust *Labeotropheus*, and distinguishes it from *L. trewavasae* and *L. rubidorsalis*, new species (Table 4). We also performed canonical discriminant function analyses on the meristic and Log<sub>10</sub>-transformed morphometric data of *L. alticodia*, *L. artatorostris*, *L. fuelleborni*, and *L. obscurus*. Both the morphometric and meristic canonical discriminant function analyses were robust and produced statistically significant results (Table 5). *Labeotropheus obscurus* is distinct from *L. artatorostris* along the first morphometric canonical function and the first meristic canonical function (Fig. 4). It is additionally distinct from *L. alticodia* and *L. fuelleborni* along the second meristic canonical function (Fig. 4).

**Distribution and abundance.**—*Labeotropheus obscurus* is endemic to the Malaŵian shore of Lake Malaŵi, and is only known from Namalenje Island. Recently, it was reported that

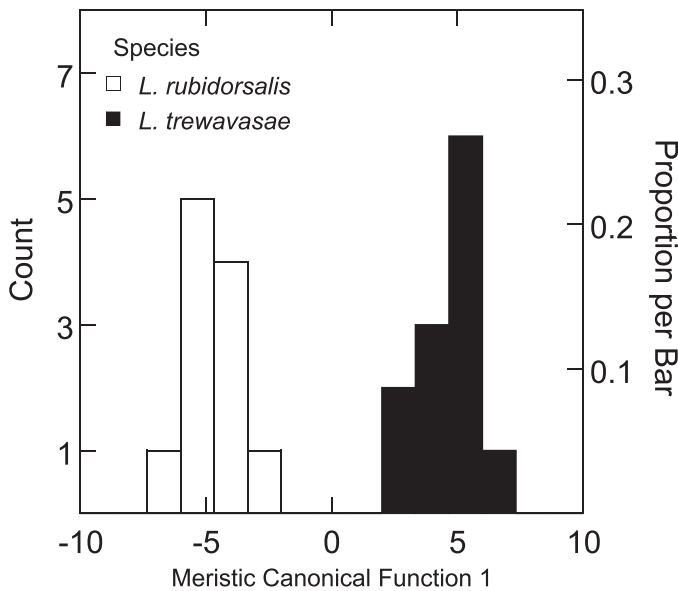


**Fig. 14.** Histogram of meristic canonical function 1 for *L. rubidorsalis* and *L. trewavasae*.

all *Labeotropheus* were possibly extirpated from Namalenje Island, as survey teams had not reported any occurrences of this genus at Namalenje Island for some time (TBP, pers. obs.). While we did both capture and observe *Labeotropheus* at Namalenje Island, females and juveniles were obvious and plentiful in the shallow regions, but males were found in deeper waters and were comparatively rare.

**Etymology.**—The specific epithet is the masculine form of the Latin adjective *obscurus*, meaning dark, dusky, or shadowy, in

reference to the muted and mostly gray male nuptial color pattern, which is unusual for a species of *Labeotropheus*.

***Labeotropheus rubidorsalis*, Phiri and Pauers, new species**

urn:lsid:zoobank.org:act:594EFD55-FB60-44DF-801F-C2B747E5865D




Figures 3, 13, 14; Tables 4, 14, 15

**Holotype.**—SAIAB 211383, adult male, 91.2 mm SL, Malaŵi, Lake Malaŵi, Maleri Island, -13.8840189, 34.6118803, Michael J. Pauers, Titus B. Phiri, and Sanudi Likupe, 16 January 2020.

**Paratypes.**—FMNH 145014, 1 male, 91.3 mm SL, 1 female, 81.6 mm SL, Malaŵi, Lake Malaŵi, Maleri Island, -13.8840189, 34.6118803, Michael J. Pauers, Titus B. Phiri, and Sanudi Likupe, 16 January 2020; MPM Fi50090, 5 females, 69.3–88.5 mm SL, Malaŵi, Lake Malaŵi, Maleri Island, -13.8840189, 34.6118803, Michael J. Pauers, Titus B. Phiri, and Sanudi Likupe, 16 January 2020; SAIAB 211382, 3 females, 67.5, 74.03, and 81.3 mm SL, Malaŵi, Lake Malaŵi, Maleri Island, -13.9089591, 34.6260792, Michael J. Pauers, Titus B. Phiri, and Sanudi Likupe, 16 January 2020.

**Diagnosis.**—*Labeotropheus rubidorsalis* differs from all other described species of *Labeotropheus* due to the nuptial color pattern of the males. The males have a vivid, almost metallic, blue head, body, and caudal peduncle, and an equally brilliant red dorsal fin. *Labeotropheus rubidorsalis* also differs from all other *Labeotropheus* by the shape of the anal fin. All other species of *Labeotropheus* have an angular to kite-shaped anal fin, but *L. rubidorsalis* has a distinctly rounded anal fin, especially in the posterior portion.

*Labeotropheus rubidorsalis* has a generally slenderer body than the most of the robust *Labeotropheus*, though its range

| Species                | Male Nuptial Color Pattern   | BD/SL Ratio                                | Distribution   |
|------------------------|--|--|--|
| <i>L. aurantinfra</i>  |  <p>Extensive orange coloration on maxilla, branchiostegals, breast, and around operculum</p> <p>Orange coloration extends dorsally across lateral line</p>           | Robust; mean BD = 36.9% of SL              | Chirwa Island<br>-10.468401, 34.281157<br>Ndomo Gap<br>-10.459141, 34.275001     |
| <i>L. chlorosiglos</i> |  <p>No orange coloration on head or breast; breast white</p> <p>Orange coloration remains ventral with respect to lateral line</p>                                    | Robust/intermediate; mean BD = 33.4% of SL | Katale Island<br>-10.455691, 34.285109<br>Makankha Reef<br>-10.456460, 34.287028 |
| <i>L. simoneae</i>     |  <p>Orange coloration on operculum; no orange on jaws, branchiostegals, or breast</p> <p>Orange coloration faint dorsally of lateral line</p> <p>Breast dark blue</p> | Slender; mean BD = 28.9% of SL             | Makankha Reef<br>-10.456460, 34.287028   |

**Fig. 15.** A comparison of the similarly colored species from the islands around the Luromo Peninsula, *L. aurantinfra*, *L. chlorosiglos*, and *L. simoneae*.

**Table 14.** Morphometric and meristic values for *Labeotropheus rubidorsalis*, new species ( $n = 11$ ).**(A) Morphometric data**

|  | Holotype | Mean±SE  | Range      |
|--|----------|----------|------------|
| Standard length (SL, mm)                                     | 91.2     | 80.3±2.5 | 67.5–91.3  |
| Head length (HL, mm)   | 26.0     | 24.4±0.6 | 21.3–27.7  |
| % SL   |          |          |            |
| HL   | 28.5     | 30.5±0.3 | 28.5–32.1  |
| Snout to origin of dorsal fin (DFO)                          | 32.4     | 33.0±0.3 | 31.4–35.0  |
| Snout to attachment of pelvic fins (PFO)                     | 37.9     | 40.2±0.6 | 37.9–43.4  |
| Length of pectoral fin                                       | 25.8     | 24.8±0.3 | 22.9–26.5  |
| Length of base of dorsal fin                                 | 62.6     | 58.7±0.5 | 56.0–62.6  |
| DFO to origin of anal fin (AFO)                              | 48.8     | 48.1±0.4 | 45.6–50.3  |
| Insertion of dorsal fin (DFI) to insertion of anal fin (AFI) | 15.3     | 14.7±0.2 | 13.5–15.7  |
| DFO to AFI   | 63.9     | 61.1±0.6 | 57.2–63.9  |
| DFI to AFO   | 30.3     | 28.9±0.2 | 27.6–30.3  |
| DFI to ventral attachment of caudal fin                      | 17.6     | 17.4±0.2 | 16.7–18.4  |
| AFI to dorsal attachment of caudal fin                       | 19.9     | 18.8±0.2 | 17.9–19.9  |
| DFO to attachment of pelvic fins                             | 33.1     | 33.0±0.3 | 31.5–35.4  |
| DFI to attachment of pelvic fins                             | 55.1     | 53.0±0.6 | 49.5–55.1  |
| Body depth   | 34.3     | 33.3±0.3 | 31.6–36.1  |
| Width at opercular tabs                                      | 17.2     | 16.5±0.2 | 14.9–17.3  |
| Width at pectoral fins                                       | 16.2     | 15.0±0.3 | 13.8–16.2  |
| Width at pelvic fins   | 7.4      | 7.3±0.1  | 6.2–8.0    |
| % HL   |          |          |            |
| Eye diameter   | 24.4     | 26.7±0.4 | 24.4–28.3  |
| Preorbital depth   | 28.0     | 29.1±0.6 | 26.6–32.9  |
| Cheek depth  | 29.5     | 27.3±0.5 | 25.1–29.6  |
| Snout length   | 30.3     | 34.2±1.1 | 29.9–42.7  |
| Rostral length   | 40.5     | 45.4±1.0 | 40.5–51.9  |
| Upper jaw length (UJL)                                       | 20.1     | 19.4±0.4 | 17.8–21.4  |
| Snout pad length   | 13.1     | 12.4±0.3 | 10.3–14.2  |
| Lower jaw length (LJL)                                       | 29.9     | 33.8±0.7 | 29.9–38.5  |
| Lower jaw width (LJW)  | 44.9     | 43.5±0.7 | 39.7–46.3  |
| Head depth   | 104.5    | 97.7±1.2 | 91.6–105.0 |
| Interorbital width   | 41.6     | 36.5±0.8 | 31.8–41.6  |
| Snout width  | 37.6     | 36.2±0.9 | 31.8–41.1  |

**(B) Meristic data**

|                                      | Holotype | Mode | Range |
|--------------------------------------|----------|------|-------|
| Anterior lateral line scales (LLS)   | 22       | 24   | 22–25 |
| Posterior LLS                        | 13       | 11   | 11–13 |
| Overlapping LLS                      | 0        | 1    | 0–3   |
| Dorso-lateral scale rows             | 10       | 9    | 8–10  |
| Pectoro-pelvic scale rows            | 10       | 10   | 10–11 |
| Cheek scale rows                     | 3        | 3    | 3–4   |
| Dorsal-fin spines (DFS)              | 18       | 18   | 17–19 |
| Dorsal-fin rays (DFR)                | 9        | 9    | 8–9   |
| Anal-fin spines (AFS)                | 3        | 3    | –     |
| Anal-fin rays (AFR)                  | 8        | 8    | 7–8   |
| Pectoral-fin rays                    | 13       | 13   | 13–14 |
| Pelvic-fin rays                      | 6        | 6    | –     |
| Upper jaw teeth rows                 | 4        | 3    | 3–4   |
| Lower jaw teeth rows                 | 5        | 4    | 3–5   |
| Teeth on left lower jaw              | 31       | 30   | 24–31 |
| Teeth on left dentigerous premaxilla | 9        | 9    | 5–12  |
| Total gill rakers                    | 10       | 10   | 9–11  |
| Epibranchial gill rakers             | 2        | 2    | 2–3   |
| Ceratobranchial gill rakers          | 7        | 7    | 5–8   |
| Infraorbital pores                   | 9        | 9    | –     |
| Neuromasts within infraorbital pores | 31       | 22   | 15–31 |



**Table 15.** Canonical discriminant function (CDF) analyses on meristic data for *L. rubidorsalis* and *L. trewavasae*; Wilks'  $\lambda = 0.038$ ,  $F_{6,16} = 66.894$ ,  $P \leq 0.001$ . Standardized functions are reported. Uninformative variables are omitted.

|                                      | CDF 1  |
|--------------------------------------|--------|
| Eigenvalue                           | 25.085 |
| Canonical correlation                | 0.981  |
| Pectoro-pelvic scale rows            | 0.720  |
| Dorsal-fin rays (DFR)                | -0.660 |
| Pectoral-fin rays                    | 1.410  |
| Upper jaw teeth rows                 | 1.175  |
| Lower jaw teeth rows                 | 1.482  |
| Teeth on left dentigerous premaxilla | -1.499 |
| Species means                        |        |
| <i>L. rubidorsalis</i>               | -4.999 |
| <i>L. trewavasae</i>                 | 4.582  |

overlaps that of several of these species (31.6–36.1% SL vs. 37.4–40.6% in *L. alticodia*, 34.3–42.0% in *L. artatorostris*, 33.8–41.5% in *L. aurantinfra*, 32.0–38.6% in *L. candipygia*, 31.9–34.7% in *L. chlorosiglos*, and 35.2–41.5% in *L. obscurus*). *Labeotropheus rubidorsalis* does have a distinctly slenderer body than some of these species as measured by the distance between the origins of the dorsal and anal fins (45.6–50.3% SL vs. 52.1–53.5% in *L. alticodia*, 50.2–58.1% in *L. artatorostris*, 51.3–54.6% in *L. chlorosiglos*, 52.5–55.5% in *L. fuelleborni*, and 50.8–56.3% in *L. obscurus*) and the insertion of the dorsal and anal fins (13.5–15.7% SL vs. 16.4–18.1% in *L. alticodia*, 15.4–18.3% in *L. artatorostris*, 15.5–16.8% in *L. chlorosiglos*, 16.5–17.4% in *L. fuelleborni*, and 15.8–17.8% in *L. obscurus*). *Labeotropheus rubidorsalis* has fewer rows of teeth in the upper jaw (3–4) than *L. artatorostris* (5–8), *L. aurantinfra* (4–6), *L. fuelleborni* (4–5), and *L. candipygia* (4–6). *Labeotropheus rubidorsalis* also has fewer rows of teeth in the lower jaw (3–5) than *L. fuelleborni* (6) and *L. chlorosiglos* (5–7).

*Labeotropheus rubidorsalis* is typically deeper-bodied than the slender-bodied *Labeotropheus* as indicated by both body depth (31.6–36.1% SL vs. 26.6–33.2% in *L. chirangali*, 26.3–33.4% in *L. trewavasae*; and 26.9–30.8% in *L. simoneae*) and by the distance between the origin of the dorsal fin and the attachments of the pelvic fins (31.5–35.4% SL vs. 28.6–33.4% in *L. chirangali*, 27.1–32.7% in *L. trewavasae*; and 27.5–32.8% in *L. simoneae*). *Labeotropheus rubidorsalis* also has fewer rows of teeth in the upper jaw than the other slender species (3–4 vs. 3–6 in *L. chirangali*, 4–7 *L. simoneae*, and 5–7 *L. trewavasae*). It also has fewer rows of teeth in the lower jaw than *L. trewavasae* (3–5 vs. 5–6).

**Description.**—Morphometric and meristic data summarized in Table 14. Body compressiform with flattened ovoid shape; body consistently deep throughout its length, especially for a slender *Labeotropheus*. Body wide, almost cylindrical in transverse cross section. Scales on belly and anterior abdomen cycloid and tightly crowded. Flank scales ctenoid; exposed portion of scale fan-shaped and approximately hexagonal. Anterior lateral line overlapping posterior lateral line by 0–3 scales. Dorsal fin long, 56.0–62.6% SL with 17–19 spines and 7–8 rays. Origin of dorsal fin posterior to or overlapping opercular tab. Dorsal-fin rays 3, 4, 5 long, reaching to hypural and beyond to caudal fin. Anal fin rounded posteriorly in all specimens. Origin of anal fin opposite dorsal-fin spine 14, 15, or 16; insertion of anal fin

anterior to insertion of dorsal fin. Anal-fin rays 3, 4, 5 reach past hypural in males; only reach to mid-caudal peduncle in females. Caudal fin subtruncate. Pectoral fin long and rounded, with 13–15 rays. Pelvic fin long, minimally reaching origin of anal fin and longer in the majority of specimens. Pelvic-fin ray slightly produced and filamentous in half of specimens; non-filamentous in other half. Pelvic-fin attachment opposite dorsal-fin spine 4, 5, or 6.

Head long and deep, especially for a slender-bodied *Labeotropheus*; head depth 91.6–105.0% HL. Head profile moderately curved with no concavity above eye. Snout long and wide with slightly protruding snout; snout pad 10.3–14.2% HL. Cheek with 3–4 scale rows. Infraorbital pores 7–9, with 8–25 neuromasts distributed among them. Oral jaws long and wide. Oral teeth tricuspid and closely set on upper and lower jaws; 5–12 tricuspid teeth on lateral portion of left upper jaw. Gill rakers stout, triangular, and widely spaced; 5–8 ceratobranchial and 2–3 epibranchial gill rakers on first gill arch. All specimens with 1 raker between the cerato- and epibranchial rakers.

**Coloration of males.**—Head, operculum, flank, caudal peduncle brilliant, solid blue; 11 faint bars spanning flank and caudal peduncle. Opercular tab faint metallic green. Dorsal fin brilliant red, fading somewhat posteriorly; small hyaline spots in rayed dorsal fin. Caudal fin same brilliant blue as rest of body, fading posteriorly, with thin red trailing edge. Spinous portion of anal fin white, becoming blue in rayed portion; 3–5 yellow eggspots present. Pelvic fin bluish white posteriorly with white leading edge, pale red between.

Preserved males uniformly gray with 11 bars faintly visible across flank and caudal peduncle.

**Coloration of females.**—Females with orange blotch ('OB') color pattern across entire body and all fins; ground color is pale orange with black, white, and darker orange spots of irregular shape and varying size. Opercular tab black or black with faint green sheen. Anal fin hyaline in some individuals, some individuals with faint orange blotches overlying hyaline anal-fin membrane. All individuals with 1–7 very small orange eggspots present on anal fin.

Preserved females uniformly white or pale gray with dark gray and/or black spots across flank and caudal peduncle.

**Multivariate analyses.**—Due to the overlap of morphometric and meristic characteristics between *L. rubidorsalis* and the other *Labeotropheus*, we compared the body depth–standard length ratios of *L. rubidorsalis* and its geographically proximate congeners (Fig. 3). This ratio shows that *L. rubidorsalis* has a body profile that is distinct from that of both the robust and slender *Labeotropheus* found nearby (Table 4). We also performed canonical discriminant function analyses on the meristic and  $\text{Log}_{10}$ -transformed morphometric data of *L. rubidorsalis* and *L. trewavasae*. While the discriminant function analysis of the  $\text{Log}_{10}$ -transformed morphometric data was not significant (Wilks'  $\lambda = 0.005$ ,  $F_{21,1} = 9.109$ ,  $P = 0.26$ ), the analysis of the meristic data was robust and significant (Table 15). When the first meristic canonical function is plotted as a histogram, *L. rubidorsalis* is clearly distinct from *L. trewavasae* (Fig. 14).

**Distribution.**—*Labeotropheus rubidorsalis* is endemic to the Malaŵian shore of Lake Malaŵi. We captured specimens at both Maleri and Nankoma Islands, in Lake Malaŵi National

Park, and found a similarly colored slender *Labeotropheus* at Namalenje Island, but only captured two specimens and did not include these in our analyses; Ribbink et al. (1983a) also reported a similarly colored slender *Labeotropheus* from Namalenje. We did not collect at the nearby Nakantenga Island, where Ribbink et al. (1983a) reported a differently colored slender *Labeotropheus*.

**Etymology.**—The specific epithet is a combination of the Latin adjective *rubi*, meaning red colored, the Latin noun *dorsum*, meaning the dorsal surface or back, and the Latin suffix *-alis*, which means pertaining to. This epithet describes the brilliant red dorsal fin of the males.

## DISCUSSION

The six species described herein more than double the number of known species of *Labeotropheus* and are thus a significant addition to the taxonomy of this genus. The inclusion of these new species is especially notable given that, until very recently, the existence of species beyond *L. fuelleborni* and *L. trewavasae* was considered virtually impossible (reviewed in Pauers, 2010). Nonetheless, Ribbink et al. (1983a, 1983b) had argued that the extensive geographic variation in male nuptial color pattern among populations of both *L. fuelleborni* and *L. trewavasae* was strong evidence for reproductive isolation among these populations, and that these differently colored, allopatric populations should be recognized as distinct species. Evidence from genetics (Arnegard et al., 1999), morphology (Pauers and McMillan, 2015; Albertson and Pauers, 2019), and behavior (Pauers et al., 2004; Pauers and McKinnon, 2012) was instrumental in providing support for re-evaluating the taxonomic status of these populations of *Labeotropheus* (Pauers, 2010, 2016, 2017).

Although *Labeotropheus* and most of the other rock-dwelling haplochromines of Lake Malaŵi are not currently considered to be threatened by the IUCN, recent publications have highlighted the threats to the continued existence of these nearshore species. Su et al. (2021) found that freshwater fishes throughout the world are vulnerable to a variety of anthropogenic stressors, exposure to which results in drastic declines in functional, taxonomic, and phylogenetic biodiversity. In Lake Malaŵi, the mbuna are at risk due to their close proximity to human settlements and activities, and their restricted distributions and stenotopic habits make them particularly susceptible to overexploitation by subsistence fishers (Kanyerere et al., 2019). Additionally, agricultural runoff degrades the rocky nearshore habitats by depositing silt and sediment on the lithophilic algae that serve as food for many of the mbuna, including *Labeotropheus* (Kanyerere et al., 2019). Interestingly, Kanyerere et al. (2019) concluded that increased and extensive taxonomic studies of the fishes of Lake Malaŵi is a vital component to their conservation and continued existence. Since the taxonomic status of many of these species, especially those with extensive geographic variation, is poorly understood, intensive ichthyological studies of these fishes could result in the description of new species. The elevation of these allopatric populations to species would allow them to be fully evaluated by the IUCN for Red List inclusion and concomitant protection. Our description of these six new *Labeotropheus* is thus an important first step in their conservation.

**On the distinctions among *Labeotropheus aurantinfra*, *L. chlorosiglos*, and *L. simoneae*.**—The islands and reefs surrounding the Luromo Peninsula seem to be a hotspot of biodiversity in the *Labeotropheus*. Given the close geographic proximity of these features, it is likely that the *Labeotropheus* that inhabit them are closely related (Arnegard et al., 1999). Although phylogeographic studies are necessary to confirm this, three of the species from this region, *L. aurantinfra*, *L. chlorosiglos*, and *L. simoneae*, reveal their possible evolutionary kinship through their strikingly similar color patterns. All three species have large orange patches along their flanks with a blue dorsum. Nonetheless, the finer details of their color patterns reveal consistent, diagnosable differences among these species (Fig. 15). For example, *L. aurantinfra* has extensive orange pigmentation on the ventral surface of the jaw, throat, and anterior abdomen, which is not found in *L. chlorosiglos* or *L. simoneae*; similarly, *L. simoneae* has orange patches on the operculum that are not found in the other two species. Additionally, these species differ in their bodily proportions, with *L. aurantinfra* having the largest body depth–standard length ratio, and *L. simoneae* the smallest. In the *Labeotropheus*, this ratio is associated with depth distribution, habitat preference, and foraging performance, and thus suggests important differences in the ecology of these species (Ribbink et al., 1983a, 1983b; Pauers et al., 2018). These differences among these species should be explored further in studies of their natural history and sexually selected behavior.

We also take the opportunity to provide further information on the type locality of *L. simoneae*. Pauers (2016) reported its type locality as a “submerged reef near Katala Island.” During our 2018 expedition to the Luromo Peninsula, we located this reef and were able to identify it as Makankha Reef, located at  $-10.4666938, 34.2874299$ . We collected several specimens of *L. simoneae* at Makankha Reef, and a few specimens of *L. chlorosiglos*.

The genus *Labeotropheus* represents an exciting opportunity to put into action the recommendations of Kanyerere et al. (2019) regarding increased taxonomic attention to the cichlids of Lake Malaŵi. Through careful and exhaustive analyses of allopatric populations of *Labeotropheus*, we hope to not only increase our taxonomic knowledge of this genus, but also to contribute to the conservation of these unique and important fishes. Nonetheless, given the degree to which morphometric and meristic characteristics can overlap among the species of *Labeotropheus*, great care must be taken to record where the specimens were collected, as well as to describe the minute details of their color patterns.

## DATA ACCESSIBILITY

Unless an alternative copyright or statement noting that a figure is reprinted from a previous source is noted in a figure caption, the published images and illustrations in this article are licensed by the American Society of Ichthyologists and Herpetologists for use if the use includes a citation to the original source (American Society of Ichthyologists and Herpetologists, the DOI of the *Ichthyology & Herpetology* article, and any individual image credits listed in the figure caption) in accordance with the Creative Commons Attribution CC BY License. ZooBank publication urn:lsid:zoobank.org:pub:E393FCFE-0ED6-466D-8D7C-2CBF9212DC1E.

## ACKNOWLEDGMENTS

Permission to conduct research in Lake Malaŵi was granted to MJP and TBP by the National Commission for Science and Technology of Malaŵi; these permits were issued on 30 July 2018 and 14 January 2020 for the respective expeditions, and we thank Yohane Chimbalanga for his assistance in acquiring these permits. Permission to collect specimens and export them to the United States was granted to MJP and TBP by the Malaŵi Department of Fisheries; these permits were issued on 17 July 2018 and 19 January 2020 for the respective expeditions, and we thank Brino Chirwa and Moffat Manase for their assistance in completing and acquiring these permits. Permission to enter Lake Malaŵi National Park and collect specimens within the park was granted to the authors on 14 January 2020 by William O. Mgoola. Permission to import these specimens to the United States was granted by the USFWS on 25 July 2018 and 6 January 2020 for the respective expeditions. For their assistance in the field in 2018, we are grateful to Victor Nantunga, Halord Bandawe, Simeon Ndomwe, and Shaibu Fisha. The Department of Fisheries and Aquatic Sciences Research at Mzuzu University provided us with formalin and alcohol for our 2018 expedition. Alfred Nyasulu provided welcome hospitality and humor, not to mention extensive advice for collecting fishes around the Luromo Peninsula, and we are thankful for his help. We remain indebted to David P. Nkhwazi for his generous assistance with an unanticipated difficulty in our 2018 expedition; our expedition would not have been possible without his kindness. Jonathan Mala and his crew were instrumental to our success in 2018, and we thank them for their diligence and professionalism. For their assistance in 2020, we thank Sanudi Likupe, Halord Bandawe, Regina Chafumuka, and Wellos Moyo.

This project was funded by the Orth Family Ichthyology Research Fund of the Milwaukee Public Museum, the former UW Colleges Summer Research Fund, the former UW-Waukesha Professional Development Fund, the UW-Milwaukee College of General Studies Professional Development Fund, the UW-Milwaukee Office of Research Travel Stipend, and the American Cichlid Association. We thank Ellen Censky (MPM) for her continued financial and administrative support of this project. We also thank Caleb McMahan (FMNH), Julia Colby (MPM), and Nkosinathi Mazungula and Roger Bills (SAIAB) for their assistance with preparing, accepting, and accessioning the type specimens; additionally, Jay R. Stauffer, Jr. assisted with delivering the types to SAIAB.

Finally, MJP would like to thank TBP for his kindness, hospitality, patience, professionalism, and his extraordinary skills as a negotiator, which solved several problems during both of our expeditions.

## LITERATURE CITED

- Ahl, E. 1927. Einige neue Fische der Familie Cichlidae aus dem Nyassa-see. *Sitzungsberichte der Berlinische Gesellschaft Naturforschender Freunde zu Berlin* 1926:51–62.
- Albertson, R. C., and M. J. Pauers. 2019. Morphological disparity in ecologically diverse versus constrained lineages of Lake Malaŵi rock-dwelling cichlids. *Hydrobiologia* 832: 153–174.
- Arnegard, M. E., J. A. Markert, P. D. Danley, J. R. Stauffer, Jr., A. J. Ambali, and T. D. Kocher. 1999. Population structure and colour variation of the cichlid fish *Labeotropheus fuelleborni* Ahl along a recently formed archipelago of rocky habitat patches in southern Lake Malawi. *Proceedings of the Royal Society B* 266:119–130.
- Barel, C., M. van Oijen, F. Witte, and E. Witte-Maas. 1977. An introduction to the taxonomy and morphology of the haplochromine Cichlidae from Lake Victoria. *Netherlands Journal of Zoology* 27:333–389.
- Conith, A. J., M. R. Kidd, T. D. Kocher, and R. C. Albertson. 2020. Ecomorphological divergence and habitat lability in the context of robust patterns of modularity in the cichlid feeding apparatus. *BMC Evolutionary Biology* 20:95.
- Dierickx, K., M. Hanssens, B. Rusuwa, and J. Snoeks. 2018. *Trematocranus pachychilus*, a new endemic cichlid from Lake Malawi (Teleostei, Cichlidae). *Zookeys* 743:153–166.
- Dierickx, K., and J. Snoeks. 2020. *Protomelas krampus*, a new paedophagous cichlid from Lake Malawi (Teleostei, Cichlidae). *European Journal of Taxonomy* 672:1–18.
- Fryer, G. 1956. A new species of *Labeotropheus* from Lake Nyasa, with a redescription of *Labeotropheus fuelleborni* Ahl and some notes on the genus *Labeotropheus* (Pisces: Cichlidae). *Revue de Zoologie et de Botanique Africaines* 54:280–289.
- Kanyerere, G. Z., T. B. Phiri, C. A. Sayer, A. Shechonge, J. Snoeks, and D. Tweddle. 2019. The status and distribution of freshwater fishes in the Lake Malawi/Nyassa/Niassa Catchment, p. 46–72. *In: Conservation Priorities for Freshwater Biodiversity in the Lake Malawi/Nyassa/Niassa Catchment*. C. A. Sayer, A. F. Palmer-Newton, and W. R. T. Darwall (eds.). IUCN, Cambridge, UK.
- Mayden, R. L. 1999. Consilience and a hierarchy of species concepts: advances toward closure on the species puzzle. *Journal of Nematology* 31:95–116.
- Oliver, M. K. 2018. Six new species of the cichlid genus *Otopharynx* from Lake Malawi (Teleostei: Cichlidae). *Bulletin of the Peabody Museum of Natural History* 59:159–197.
- Oliver, M. K., and M. E. Arnegard. 2010. A new genus for *Melanochromis labrosus*, a problematic Lake Malawi cichlid with hypertrophied lips (Teleostei: Cichlidae). *Ichthyological Exploration of Freshwaters* 21:209–232.
- Pauers, M. J. 2010. Species concepts, speciation, and taxonomic change in the Lake Malawi mbuna, with special reference to the genus *Labeotropheus* Ahl 1927 (Perciformes: Cichlidae). *Reviews in Fish Biology and Fisheries* 20:187–202.
- Pauers, M. J. 2016. Two new and remarkably similarly colored species of *Labeotropheus* (Perciformes: Cichlidae) from Lake Malaŵi, Africa. *Copeia* 104:628–638.
- Pauers, M. J. 2017. A new species of *Labeotropheus* (Perciformes: Cichlidae) from southern Lake Malaŵi, Africa. *Copeia* 105:399–414.
- Pauers, M. J., K. R. Fox, R. A. Hall, and K. Patel. 2018. Hybridization, selection, and the evolution of morphology in the Lake Malaŵi endemic cichlids of the genus *Labeotropheus*. *Scientific Reports* 8:15842.
- Pauers, M. J., and J. S. McKinnon. 2012. Sexual selection on color and behavior within and between cichlid populations: implications for speciation. *Current Zoology* 58:472–480.
- Pauers, M. J., J. S. McKinnon, and T. J. Ehlinger. 2004. Directional sexual selection on chroma and within-pattern contrast in *Labeotropheus fuelleborni*. *Proceedings of the Royal Society B (Supplement)* 271:S444–S447.



- Pauers, M. J., and S. A. McMillan.** 2015. Geometric morphometrics reveals surprising diversity in the Lake Malawi cichlid genus *Labeotropheus*. *Hydrobiologia* 748: 145–160.
- Ribbink, A. J., A. C. Marsh, B. A. Marsh, and B. J. Sharp.** 1983b. The zoogeography, ecology and taxonomy of the genus *Labeotropheus* Ahl, 1927, of Lake Malawi (Pisces: Cichlidae). *Zoological Journal of the Linnean Society* 79: 223–243.
- Ribbink, A. J., B. A. Marsh, A. C. Marsh, A. C. Ribbink, and B. J. Sharp.** 1983a. A preliminary survey of the cichlid fishes of rocky habitats in Lake Malawi. *South African Journal of Zoology* 18:149–310.
- Sabaj, M. H.** 2020. Codes for natural history collections in ichthyology and herpetology. *Copeia* 108:593–669.
- Sayer, C. A., A. F. Palmer-Newton, and W. R. T. Darwall (Eds.).** 2019. Conservation Priorities for Freshwater Biodiversity in the Lake Malawi/Nyasa/Niassa Catchment. IUCN, Cambridge, UK.
- Simpson, G. G.** 1961. Principles of Animal Taxonomy. Columbia University Press, New York.
- Stauffer, J. R., Jr.** 2018. Description of *Metriaclima koningsi*, a new species (Teleostei: Cichlidae) from Lake Malawi, Malawi, Africa. *Zootaxa* 4370:95–100.
- Stauffer, J. R., Jr., R. Bills, P. H. Skelton, and O. L. F. Weyl.** 2020. Re-elevation to species level and redescription of *Serranochromis jallae* and *Serranochromis robustus* (Teleostei: Cichlidae). *Zootaxa* 4858:126–134.
- Stauffer, J. R., Jr., N. J. Bowers, K. A. Kellogg, and K. R. McKaye.** 1997. A revision of the blue-black *Pseudotropheus zebra* (Teleostei: Cichlidae) complex from Lake Malawi, Africa, with a description of a new genus and ten new species. *Proceedings of the Academy of Natural Sciences of Philadelphia* 148:189–230.
- Stauffer, J. R., Jr., and A. F. Konings.** 2021. A new species of *Diplotaxodon* (Cichliformes: Cichlidae) from Lake Malawi. *Zootaxa* 4903:275–284.
- Stauffer, J. R., Jr., and K. A. McKaye.** 2001. The naming of cichlids. *Journal of Aquaculture and Aquatic Sciences* 9: 1–16.
- Stauffer, J. R., Jr., T. B. Phiri, and A. F. Konings.** 2018. Description of two deep-water fishes of the genus *Diplotaxodon* (Teleostei: Cichlidae) from Lake Malawi, Africa. *Proceedings of the Biological Society of Washington* 131: 90–100.
- Su, G., M. Logez, J. Xu, S. Tao, S. Villéger, and S. Brosse.** 2021. Human impacts on global freshwater fish biodiversity. *Science* 371:835–838.
- Weyl, O. L. F., A. J. Ribbink, and D. Tweddle.** 2010. Lake Malawi: fishes, fisheries, biodiversity, health and habitat. *Aquatic Ecosystem Health and Management* 13:241–254.
- Wiley, E. O.** 1978. The evolutionary species concept reconsidered. *Systematic Zoology* 27:17–26.